5

CASE STUDY OF A BORANE–THF EXPLOSION

David J. am Ende*
Nalas Engineering Services, Inc., Centerbrook, CT, USA

Richard M. Davis
Global Environmental, Health and Safety, Pfizer, Inc., Groton, CT, USA

5.1 INTRODUCTION

Borane–THF (BTHF) is a specialty chemical supplied as a solution in tetrahydrofuran (THF) often used in pharmaceutical research and industrial applications as a reducing agent for aldehydes, ketones, amides, and other functional groups [1]. In 2002, a large cylinder of BTHF experienced a boiling liquid expanding vapor explosion (BLEVE) upon storage at Pfizer's R&D site in Groton, CT. This chapter provides a case study specific to the thermochemical aspects of BTHF, its storage condition and how the analysis ultimately provided understanding into the cause of the explosion.

5.2 BACKGROUND

The original lot of six cylinders of BTHF, each with a capacity of 400 L (350 kg) was purchased with the intention to be used in a pilot plant campaign to perform a chemical reduction step in the synthesis of a drug candidate. The cylinders were shipped from the manufacturer on 4 March 2002 and delivered to Pfizer R&D (Groton, CT) on 6 March 2002 and placed in one of Pfizer's flammable materials storage buildings external to the site's pilot plant. A little less than four months after receiving the cylinders, on 25 June at 8:00 a.m., one of the six cylinders exploded, resulting in a large fire ball and significant structural damage to the warehouse and adjacent buildings. Multiple injuries were suffered as well [2]. The bottom of the exploded drum is shown in Figure 5.1. The type of explosion that occurred was ultimately classified as a BLEVE. A BLEVE occurs when a tank containing a liquid held above its normal boiling point ruptures, resulting in the explosive vaporization of the tank contents, and when the vaporized liquid is flammable, can result in a vapor cloud explosion. [3] The focus of this case study is on the technical details and analysis with worked out example problems and calculations used to help understand the cause of the thermal runaway reaction. It is intended as a process safety educational tool to highlight the challenges and approaches to thermal characterization of reactive materials, with respect to added stabilizers, and their packaging configurations and storage conditions.

BTHF solution is typically prepared industrially by dissolving diborane gas into THF. A small amount of additive such as sodium borohydride, $NaBH_4$, is typically added to the solution as a stabilizer [4]. The stabilizer is used to slow the rate of decomposition that occurs by ether cleavage, leading to loss of purity of BTHF as shown in Scheme 5.1.[1]

The decomposition pathway occurs through ring opening of the THF and is assumed to proceed through monobutoxyborane (M). Since [M] is not actually observed, it is assumed to be short-lived, rapidly disproportionating, so

*Previous address: Chemical R&D, Pfizer, Inc., Groton, CT, USA

[1]Borane-Tetrahydrofuran 1 and 2 M Solutions, manufactured by Callery Chemical Company, Division of Mine Safety Appliances Co., MSDS dated 22 March 2001.

Chemical Engineering in the Pharmaceutical Industry: Active Pharmaceutical Ingredients, Second Edition.
Edited by David J. am Ende and Mary T. am Ende.

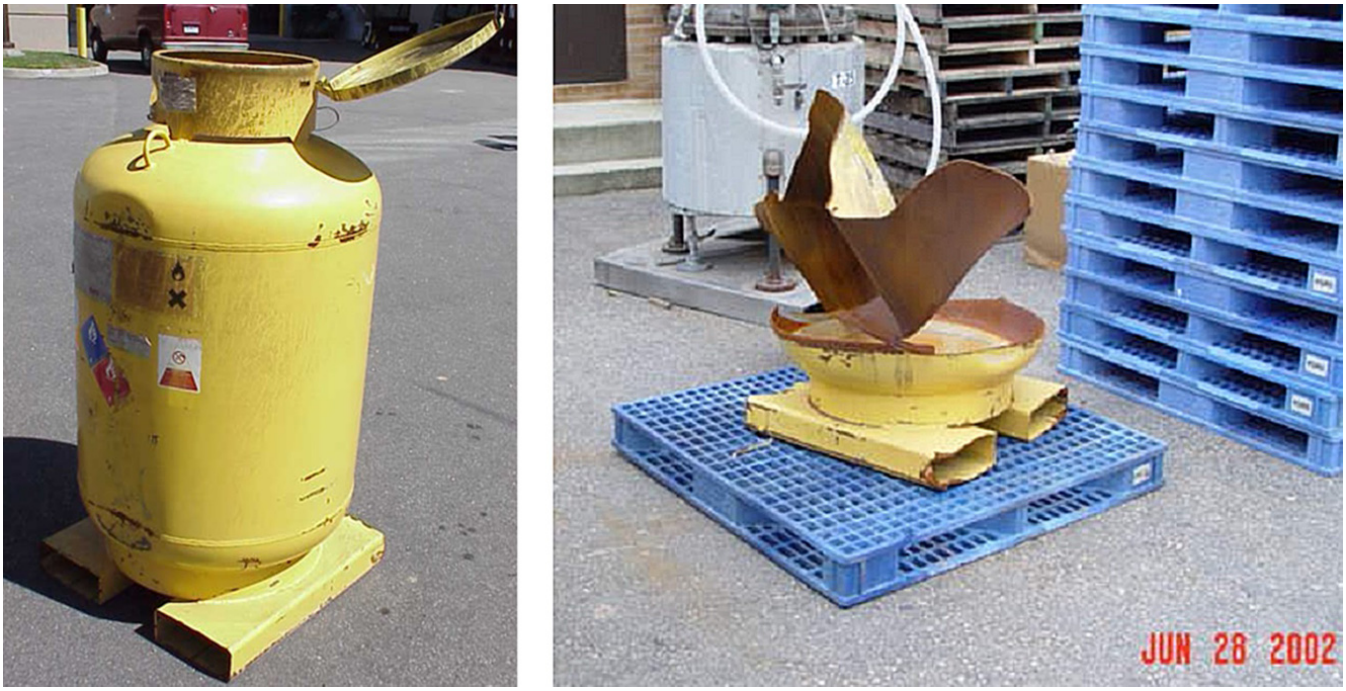

FIGURE 5.1 One of the unbreached 400 L cylinders of BTHF remaining after the explosion (left). The base of the cylinder impacted by the BLEVE recovered after the explosion (right).

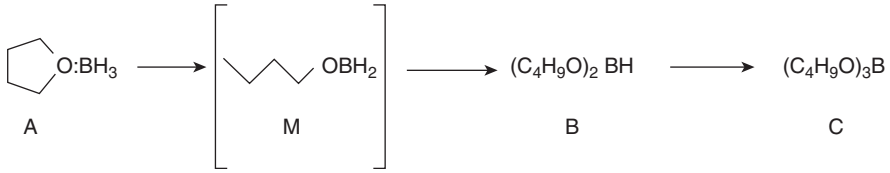

SCHEME 5.1 BTHF decomposition via ether cleavage: borane–THF (BTHF) [A], mono-butoxyborane [M], dibutoxyborane [B], and tributyl borate [C].

the rate to form [B] from [M] is considered fast. More detailed kinetic analysis and modeling, based on a slightly more complex mechanism, is described later in this case study. As the material ages, especially at ambient temperatures, this ring-opening decomposition leads to a loss of potency of BTHF with accumulation of species B and C as shown in Scheme 5.1.

The stabilizer slows the ring-opening decomposition, but the exact mechanism of how the sodium borohydride inhibits the ring opening is not well understood. More recently new stabilizers have been developed, claiming improved thermal properties and stability of BTHF solutions [5]. Flanagan and coworkers have recently published on safe handling of 1 M solutions [6]. For this case study, however, our focus is on sodium borohydride-stabilized solutions of BTHF with concentrations between 1 and 2 M solution.

Chemical stability data obtained from *isothermal* studies indicated that the material loses potency at a rate that depends on temperature. Thus the storage condition recommended by the manufacturer was to store cold (at 0 °C or lower) to protect product purity. There was no adiabatic test data or self-accelerating decomposition temperature (SADT[2]) determinations specific to the packaging configuration (e.g. 400 L cylinders containing 2M BTHF).

At the time of the incident, there were six cylinders of BTHF stored inside the flammable materials warehouse adjacent to the pilot plant. On the day of the incident, one cylinder exploded, and a second one was breached (by the explosion of the first cylinder), while the remaining four cylinders remained intact. After the explosion, the remaining four cylinders were measured to have elevated temperatures and pressures. As part of the emergency response, the cylinders were sprayed with water and packed with ice. Pressure gauges were installed on the cylinders to monitor any further

[2]SADT refers to self-accelerating decomposition temperature.

buildup of pressure. Technical representatives from the manufacturer arrived on-site to provide consultation for handling the remaining cylinders.

In addition to injuries to personnel and damage to buildings, the incident resulted in closure of the R&D site, employing approxiamtely 5000, for approximately 5 days until the remaining cylinders could be safely transported off-site to the manufacturer.

5.3 INVESTIGATION

One facet of the investigation focused on the thermochemical stability of the material.

Once it was determined that a cylinder of BTHF exploded, there were many questions as to why it happened. Was this material actually BTHF? Was it contaminated? Why did only one cylinder explode? What was the cause?

One of the first items to be established was the chemical composition of the BTHF in the unbreached cylinders. It was important to understand whether it was typical or atypical and if there was any suspected type of contamination that may have altered its stability.

A sample was obtained from one of the four surviving cylinders. Boron NMR (^{11}BNMR) was one of the tests used for confirming the identity and composition of the BTHF in the cylinder. The ^{11}BNMR spectrum of the sample confirmed the identity of the material (i.e. the material was indeed BTHF), and the spectrum is shown in Figure 5.2.

EXAMPLE PROBLEM 5.1

A liquid sample was withdrawn from one of the surviving cylinders recovered post-incident. It was found to have a ^{11}BNMR spectrum with the integral data for the three major components as shown in Figure 5.2.

Assuming the original potency was 2.0 M BTHF (in solution with THF) and using the NMR data:

(a) Calculate the molarity of BH_3-THF complex remaining in the cylinder.
(b) Calculate the molarity of active hydride "B-H" species.
(c) A hydrogen evolution test showed that a 5.0 ml of sample of the BTHF sample injected into a large excess of methanol liberated 535 ml (at 25 °C) of hydrogen (via an inverted graduated cylinder and measuring the displacement of water). Calculate the active hydride and compare the result with the molarity calculated from NMR results in part (b).

Solution

(a) There is only one boron in each of the species, so Integral% = mol % in this case; using the data from Figure 5.2, calculate the relative mol %:

$$\frac{3.6751}{1.000+3.6751+0.9385}=\frac{3.6751}{5.6136}=65.5\,\text{mol}\%\text{BH3}-\text{THF}$$

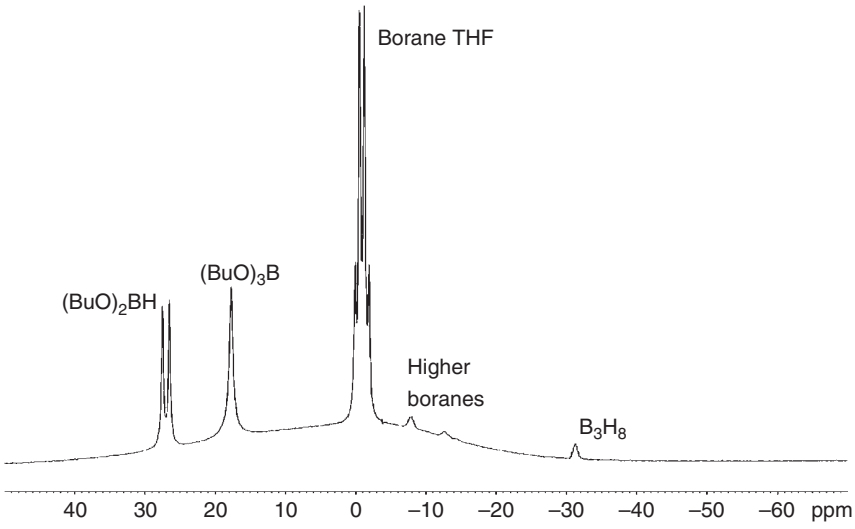

Species	^{11}B NMR Integral
Borane-THF BH_3-THF	3.6751
Dibutoxyborane $(BuO)_2BH$	1.0000
Tributylborate $(BuO)_3B$	0.9385

FIGURE 5.2 ^{11}BNMR spectrum obtained from cylinder 24 893 tested showed partial decomposition of BTHF to dibutoxyborane and tributoxyborane. Insets are the respective integrals for the three major components.

- Dibutoxyborane = $\frac{1.000}{5.6136} = 17.8\,\text{mol\%}\ (\text{BuO})_2\text{BH}$
- Tributyl borate = 16.7 mol % $(\text{BuO})_3\text{B}$
- If the original potency was 2.0 M, the new potency is 65.5% × 2 M = 1.31 M BH3-THF. Similarly, the concentration of dibutoxyborane is 0.36 M, and tributyl borate is 0.33 M.

(b) BH_3 contributes three hydrides, while dibutoxyborane only contributes one. Tributyl borate contributes no active hydride.

- Mols of active "B-H" hydrides:

$$\frac{[(3)\times 65.5\% + (1)\times 17.8\% + (0)\times(16.7)]}{100} = 2.143$$

- Theoretical mols "B-H" hydride per mol of BH3-THF = 3.0
- Active hydride:

$$\% = \frac{2.143}{3.0} = 71.4\,\text{mol\%}$$

- Remaining molarity of active hydride:

$$2\,\text{M} = 2.0\times 71.4\% = 1.43\,\text{M active hydride}$$

(c) The methanol rapidly quenches BTHF releasing hydrogen gas.

$$\text{THF}\cdot\text{BH}_3 + 3\text{MeOH} \rightarrow 3\text{H}_2 + (\text{OMe})_3\text{B} + \text{THF}$$

- Liquid sample = 5.0 ml of BTHF sample
- Mols gas liberated = $535\,\text{ml}\times\frac{\text{mol H}_2}{22\,400\,\text{ml H}_2}\times\frac{273\,\text{K}}{298\,\text{K}} = 0.0219\,\text{mol H}_2$
- Overall potency of hydride:

$$0.0219\,\text{mol H}_2\ \text{liberate}\times\frac{\text{mol BTHF}}{3\,\text{mol H}_2}*\frac{1}{0.0051} = 1.46\,\text{M active hydride}^{\text{"B-H"}}$$

- 1.46 M compares closely to the calculated 1.43 M hydride potency from NMR and provides two independent checks on the potency of active hydride.

These results revealed that the contents were indeed BTHF. There were other factors studied, including metallurgical studies on the cylinder, but in the final analysis, there was nothing to suggest chemical contamination or issue with the materials of construction. Further, the BTHF potency had diminished in potency by approximately 30%, forming typical ring-opening components, as would be expected, and so its concentration did not appear to be atypical. The BTHF manufacturer also tested the contents of each of the returned cylinders, and their data also supported this conclusion that the material, although aged with some loss of potency, otherwise appeared normal.

5.4 ARC DATA OF BTHF FROM AN ADJACENT CYLINDER

Accelerating rate calorimetry (ARC) is able to provide information on thermal runaway behavior of substances and reaction mixtures. It is considered an industry standard test for the determination of thermal stability and specifically, self-heating characteristics of materials [7]. The ARC uses a *heat–wait–search (HWS)* cycle where it first *heats* the sample to the starting temperature and then *waits* for a set period and then *searches* for an exotherm. If the exotherm in any cycle exceeds a certain threshold during the search period, an "exotherm" is detected. If an exotherm does not exceed the threshold, the ARC will heat the sample incrementally (typically 5 °C) to the next plateau.

A sample obtained from one of the adjacent cylinders post-incident was tested using ARC. The composition of this sample was 1.3 M BTHF and 1.46 M active hydride (71% of original), having lost 29% potency of active hydride due to the extended storage time under ambient conditions.

A photo of the ARC system is shown in Figure 5.3. The ARC results are shown in Figures 5.3 and 5.4 from recovered sample cylinder #24893. In Figure 5.3 both temperature and pressure are profiled as a function of time. The pressure reaches 500 psi, and the temperature reaches over 190 °C due to self-heating (with no phi correction). In Figure 5.4, the self-heat rate data are plotted. These data are logged during exotherm mode, and it shows a self-heat rate (uncorrected for PHI) of approximately 4 °C/min and an uncorrected adiabatic temperature rise of 140 °C. The PHI factor for the sample was 2.4.[3] An independent validation of the PHI factor was performed to justify this more conservative PHI factor and is described in Appendix 5.A. After correcting for PHI, the adiabatic temperature rise, even from this relatively low potency of 1.3 M, was 336 °C (i.e. $\Delta T_{ad}\cdot\varphi = 140\cdot 2.4$). Refrigerated 2 M BTHF from the same lot retained by the manufacturer was tested and was shown to have an adiabatic temperature rise above 500 °C due to its higher potency.

From Figure 5.4, the ARC detects an "exotherm" on the second temperature step based on the strict criterion of detected self-heat rate greater than 0.02 °C/min.

[3]The phi factor is a measure of the thermal mass of the sample and container relative to the sample alone and is calculated from $\varphi = [(mCp)_{\text{sample}} + (mCp)_{\text{cell}})]/(mCp)_{\text{sample}}$. The borane THF sample was 4.357 g; the cell was a 10.3810 g titanium ARC cell with fittings weighting 10.7730 g. The calculated phi factor for the sample and test cell (no fittings) was 1.57. The calculated PHI for the sample and test cell with fittings was 2.40.

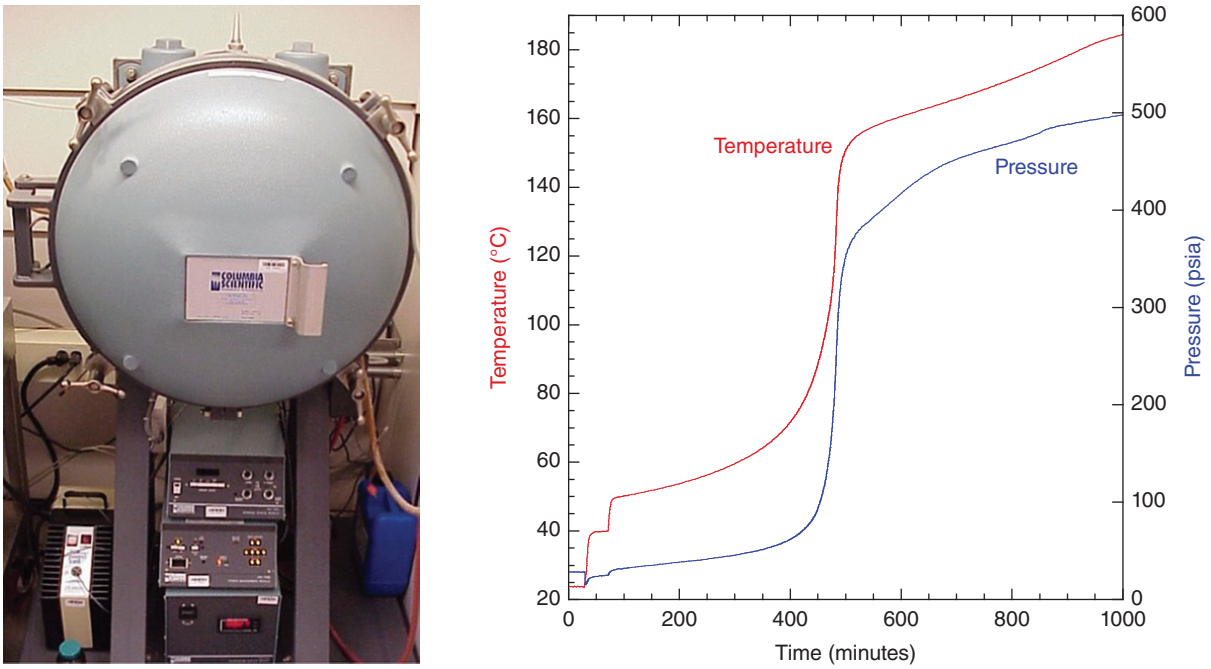

FIGURE 5.3 Left: accelerating rate calorimeter (Columbia Scientific). Right: heat–wait–search profile ARC experiment on "aged" BTHF recovered from a surviving cylinder. The composition was 1.46 M "B-H" active hydride B-H and 1.3 M BH_3-THF.

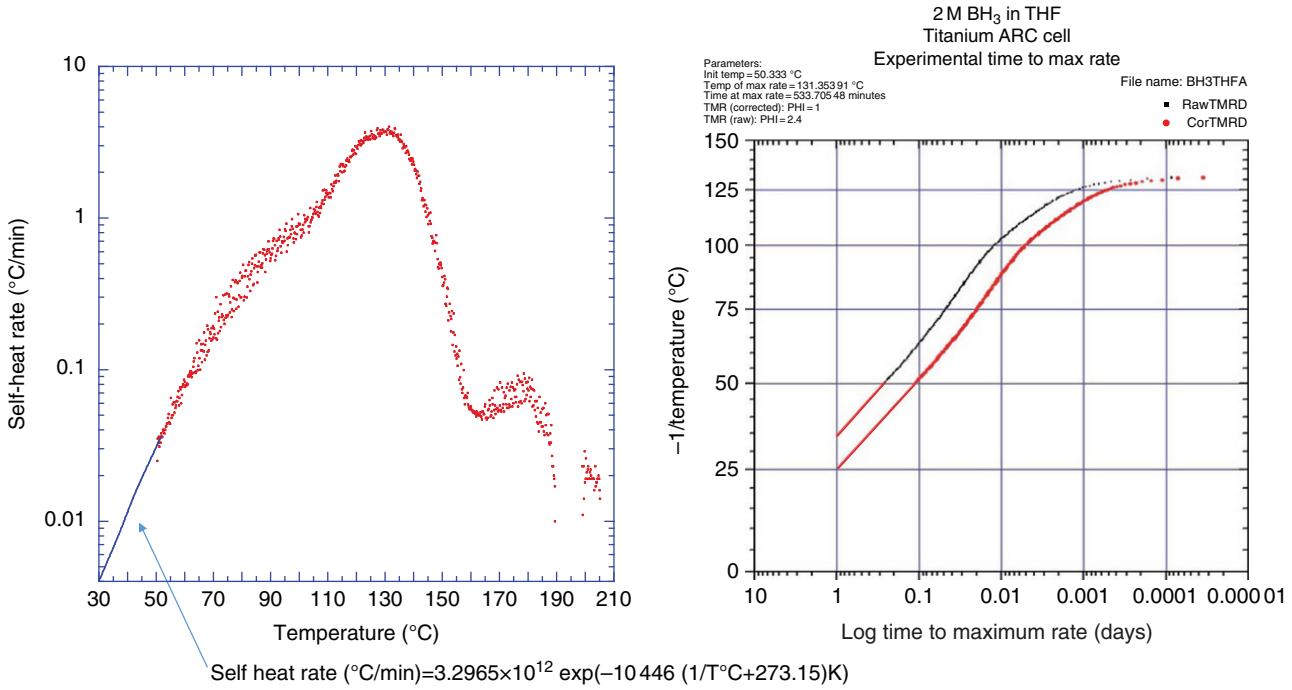

FIGURE 5.4 Left: self-heat rate curve of aged BTHF. Right: time to maximum rate plot for aged BTHF (1.3 M BH_3-THF).

However, it actually was self-heating before 50 °C, but in the HWS method, the ARC had to finish the step before it transitioned into exotherm mode. This is evident from the curve since the exotherm threshold was 0.02 °C/min, but the first data point was closer to 0.03 °C/min (initial points from Figure 5.4). The solid line on the self-heat rate curve (between 30 and 50 °C) was extrapolated from the regression analysis of the initial self-heat data, resulting in the following equation:

$$\text{Self-heat rate}\,(^\circ\text{C/min}) = 3.2965 \times 10^{12} \times \exp(-10\,446\,(1/\text{T}^\circ\text{C} + 273.15)\text{K}) \quad (5.1)$$

The regression is in the form of Arrhenius equation and will be used for calculating the heat generation rate and SADT later in this chapter.

The maximum self-heat rate is literally at the peak of the self-heat rate vs. temperature plot shown in Figure 5.4. The ARC data can easily be analyzed to calculate the time to maximum rate (TMR) from each temperature. The TMR data are shown in Figure 5.4 (right). By extrapolating the TMR curve, an estimate for TD24 can be made where TD24 is the temperature where the TMR is 24 hours when held under adiabatic conditions. Graphically the phi-corrected TD24 is near 25 °C for this age and potency of BTHF.

TMR can also be calculated from Eq. (5.2) [8]:

$$\text{TMR} = \frac{C_\text{p} R\, T_\text{o}^2}{q_\text{o} E_\text{A}} \quad (5.2)$$

where

TMR = time to maximum rate, seconds

Cp = heat capacity of the material (BTHF), J/(kg·K)

R = gas constant, J/molK

T_o = initial temperature of the runaway

q_o = heat release rate, W/kg at T_o

E_A = activation energy, J/mol

EXAMPLE PROBLEM 5.2

1. Using Eq. (5.2), calculate the TMR for four *initial* temperatures: 20, 25, 27, and 30 °C; use the heat generation rate, q_o, Eq. (5.1). Assume Phi = 2.4 for correcting the heat generation rate. Assume Cp = 1740 J/kg K.
2. Now find the TD24 (hint: find the temperature where TMR = 24 hours).
3. Using the same equation, find the effect of the PHI correction on the calculated TD24's for PHI corrections of 1.0 (i.e. no correction), 1.57, 2.0, and 2.4.

Solution

1. Set up a spreadsheet and calculate as follows:

°F	TD24 (°C)	Self Heat Rate (°C/min) Eq. (5.1)	phi Correction	Heat Release q_o (W/kg)	TMR (s)	TMR (h)
68	20	0.001103	2.4	0.076766443	186 469.4	51.80
77	25	0.0020049	2.4	0.124190015	106 113.9	29.48
80.6	27	0.0025321	2.4	0.156846833	85 151.1	23.65
86	30	0.0035732	2.4	0.221335451	61 553.6	17.10

where

"self-heat rate" = $(3.2965 \times 10^{12}) \times \exp(-10\,446/(^\circ\text{C} + 273.15)) \equiv ^\circ\text{C/min}$

And "heat release rate" = PHI × (self-heat rate)(1740 J/kg K)/(60 s/min) ≡ W/kg

And TMR = $(1740 \times (^\circ\text{C} + 273.15)^2)/(\text{heat release} \times 10\,446) \equiv$ seconds.

Note 10 446 = E/R.

The results show that TMR at 20, 25, 27, and 30 °C is 51.8, 29.5, 23.65, and 17.1 hours, respectively. These data suggest that under these conditions, the TMR is less than 24 hours starting from 27 °C. It should be noted that this result is specific to this age and composition of BTHF under adiabatic conditions; nevertheless it is a surprisingly low value of TD24.

2. Using the same spreadsheet, iterate the temperature until TMR = 24 hours; we find more precisely TD24 = 26.85 °C.
3. Similarly, input the phi corrections, and iterate temperature until TMR = 24 hours. We find TD24 ranging from 26.85 to 35.1 °C – all within the range of ambient temperatures.

°F	TD24 (°C)	Self Heat Rate Eq. (5.1)	phi Correction	q_o at 25 (W/kg)	TMR (s)	TMR (h)
80.3	26.85	0.0024884	2.4	0.173192	86 559	24.04
87.4	30.8	0.0039124	1.57	0.158536	86 391	24.00
95.2	35.1	0.006319	1	0.163093	86 369	23.99
83.3	28.5	0.0030105	2	0.155401	86 804	24.11

Based on the calculations and the graphical data, the TD24, under adiabatic conditions, was in the range of 25–27 °C for this potency. These TD24's were surprising low as it suggested runaway behavior is expected at ambient temperatures under adiabatic (well-insulated or low heat loss) conditions. This was a significant finding in the investigation.

Reiterating, the TD24 is the temperature under adiabatic conditions where the maximum rate is achieved over a 24 hour period. For designing safe processes in the kilo lab or pilot plant, it is good practice to characterize TD24 and to ensure temperatures are typically controlled to well below TD24. TD24 is useful because it provides a 24 hour "window" to respond if a rise in temperature is detected. Although since these cylinders were not continuously monitored, with the information developed as part of the investigation, it should be obvious to the reader that a TD24 anywhere near ambient temperatures for these cylinders turned out to be a serious safety concern. Values this low, if previously known, would have signaled the need for refrigeration for safety reasons. Specifically the TD24 values were in the range of 25–27 °C for this age and relatively low potency of BTHF. It is likely the TD24 is even lower for higher potency BTHF that have become unstabilized during aging. The ambient temperature the day prior to explosion reached 29–30 °C.

Under US Department of Transportation (DOT) regulations, shipment of a package at ambient temperature containing self-reactive materials with an SADT of less than or equal to 50 °C is prohibited unless the material is sufficiently stabilized or inhibited (Potyen et al. [6]). The SADT also depends on the specific packaging, in this case a 400 L cylinder, so information about heat transfer from a filled cylinder is necessary to properly assess the SADT. This will be discussed in a later section.

Based simply on this ARC experiment, the extrapolated data suggested there was a previously unknown but significant thermal runaway potential for this material even at ambient temperatures. In addition, the kinetics of decomposition, based on self-heat rate vs. temperature, appear to follow first-order kinetics. As such there appears to be little or no effect of stabilizer remaining. Further it was suggested that aged BTHF solutions, like those held under ambient conditions in the flammable materials warehouse, eventually became effectively unstabilized. Confirmation was made by preparing laboratory scale BTHF from diborane gas and THF, without stabilizer, and comparing the self-heat rates with those samples pulled from the cylinders remaining after the incident. This is shown in Figure 5.5. The concentrations of BTHF are slightly different (1.3 vs. 1.5 M potency), but the initial rates were similar, indicating that *aged* BTHF essentially behaves as *unstabilized* BTHF. The effect of time–temperature history on loss of stabilizer and temperature stability will be discussed in more detail in later sections.

5.5 TEMPERATURE HISTORY OF THE BORANE–THF CYLINDERS

A batch of stabilized BTHF (Lot # 385765) was manufactured on 1 March 2002, and 6 cylinders each containing 350 kg of 2 M BTHF solution (~400 L per cylinder) were

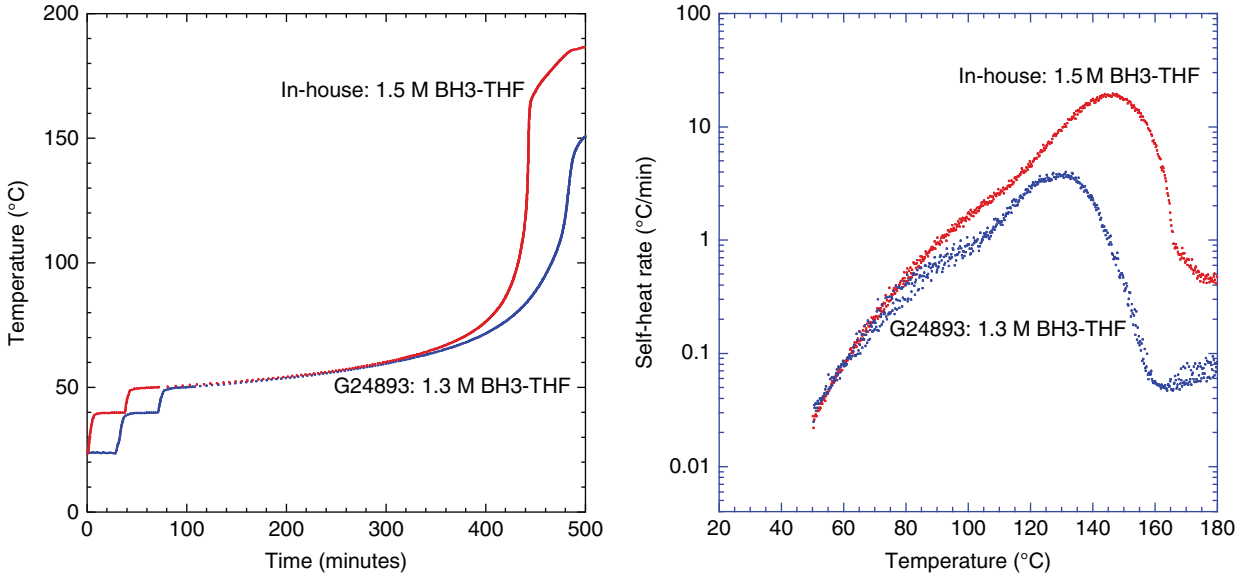

FIGURE 5.5 ARC data comparing aged BTHF G24893 to laboratory-prepared *unstabilized* BH3-THF of similar potencies. The unstabilized BTHF was prepared at laboratory scale by bubbling diborane gas into neat THF.

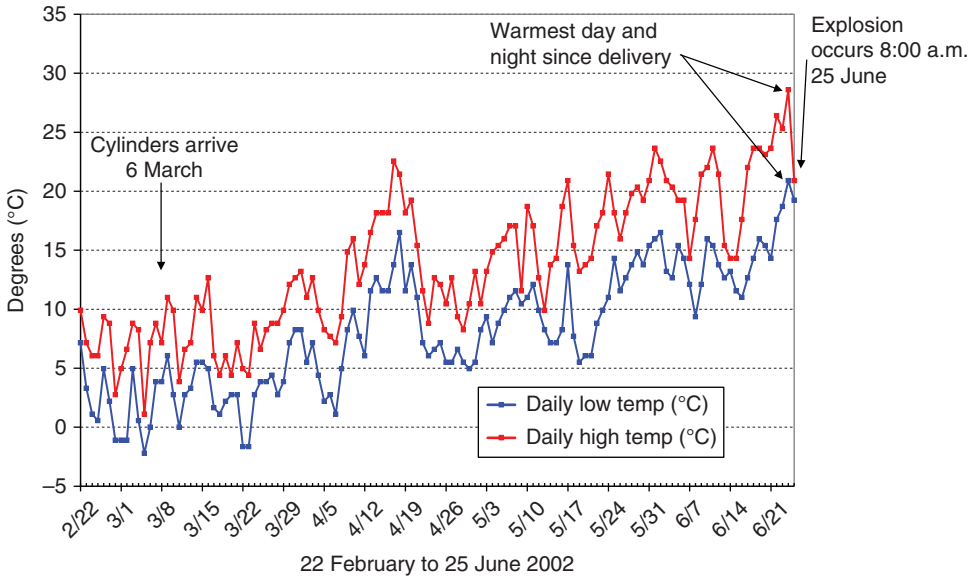

FIGURE 5.6 Daily high and low temperature readings during storage of BTHF cylinders in the warehouse.

filled at the manufacturer. The six cylinders were transported by truck (unrefrigerated) to Groton, CT. Several other cylinders were filled on the same day from the same lot and were retained at the manufacturer. The six cylinders arrived at Pfizer's, R&D site in Groton, CT, on 6 March 2002 and placed into the flammable materials warehouse. Temperatures in the warehouse were maintained at ambient temperatures using ventilation fans, and interior temperatures were recorded via a chart recorder. With the exception of a few hours when the cylinders were moved outside to perform warehouse housekeeping, the six cylinders remained in the building from 6 March to 25 June 2002 (112 days).

As seen from Figure 5.6, there was a gradual seasonal warming trend between March and June, as would be expected. Interestingly, the day before the incident, the high reached 84 °F (29 °C) by 4:00 p.m. and remained warm during the overnight hours, only dropping to 70 °F (21 °C). Both of these temperatures (high and low) in the warehouse were the warmest during the 112 day storage period. In fact, it was the first time during the entire storage period that there was a sustained temperatures above 20 °C for 24 hours. The average outside temperature for the local area for the 24 hours before the explosion was 75.7 °F (24.3 °C) based on local weather station data.

On 25 June at 7:58 a.m., minutes before the explosion, an employee observed that the cylinder exterior surface was smoking, smelled burning paint, and felt radiant heat from the cylinder. The employee also observed that the cylinder had become misshapen, described as football shaped. Two minutes later, at 8:00 a.m., the BLEVE occurred.

5.6 HEAT LOSS MEASUREMENTS

To understand the role of the storage container on the storage and shipping of two molar BTHF, Pfizer obtained a nearly identical, new, empty 400 L cylinder from a cylinder manufacturer to perform heat loss experiments. As a first trial, the cylinder was filled with hot water from a separate tank. Since the liquid was uniformly heated in the separate vessel, initial temperature gradients could be avoided (compared with heating the cylinder externally with a drum heater). Once the cylinder was filled with water, it was weighed again. Thermocouples were placed in the cylinder and on the side wall to record and log temperature data. For the cooling experiment, the cylinder was positioned on a pallet on the floor and was simply allowed to cool while logging the internal cylinder temperature with time. The setup is shown in Figure 5.7.

Passive cooling experiments with THF were also performed. THF is a good model for temperature experiments simulating 2 M BTHF.[4] THF was heated in a stirred tank to nearly 60 °C. The cylinder was inerted with nitrogen, vented, and grounded, and the THF was transferred to the cylinder. Once the liquid was transferred to the cylinder, the valve was closed. The temperature data were logged, while the cylinder cooled under an ambient temperature of 22 °C. The cooling data from each of the experiments is shown in Figure 5.8.

The cooling data were numerically regressed, resulting in the following equations for water and THF, respectively:

[4]Since BTHF is a solution in THF, the properties of THF are a good assumption – thus the heat capacity and thermal conductivity are expected to be very similar.

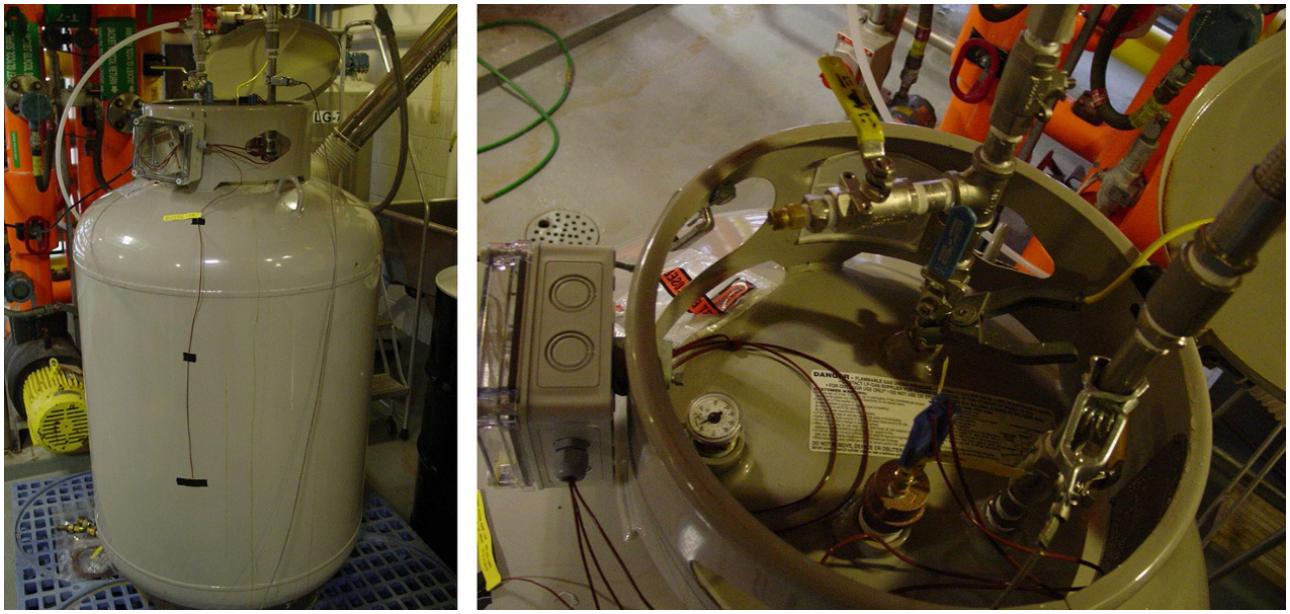

FIGURE 5.7 An identical, new, empty 400 L carbon steel cylinder. The cylinder was equipped with internal thermocouples and filled to perform a passive cooling experiment to determine the rate of heat loss from a typical 400 L steel cylinder.

$$\text{Water}: T(t) = 22^{\circ}\text{C} + 37.919\exp(-0.001\,043\,6 \times t) \quad (5.3)$$

$$\text{THF}: T(t) = 22^{\circ}\text{C} + 29.082\exp(-0.002\,325\,3 \times t) \quad (5.4)$$

where t is in minutes. These fits of course are based on Newton's law of cooling equation:

$$T(t) = T_{\text{final}} + (T_{\text{initial}} - T_{\text{final}})\exp((-hA/mCp) \times t) \quad (5.5)$$

The curve fits are described in more detail in Example Problem 5.3.

EXAMPLE PROBLEM 5.3

Two passive cooling experiments were performed in a 400 L steel cylinder. The temperature data are plotted from each cooling experiment as shown in Figure 5.8 below. The data were regressed via nonlinear curve fit of the form shown in Eqs. (5.3), (5.4), and (5.5):

1. Derive Eq. (5.5) from Newton's law of cooling.
2. Using the regression coefficients from the curve fits, estimate a lumped parameter heat transfer coefficient for the convective cooling of the 400 L cylinder for both water and THF. Assume:
   - Cylinder containing water: 350 kg of water; *Cp* Water = 4.18 J/(g·K)
   - Cylinder containing THF: 333 kg of THF; *Cp* THF = 1.765 J/(g·K)
3. Estimate the PHI factor for the 400 L cylinder filled with BTHF.

Additional tank specifications:

1000# DOT cylinder
Working pressure = 240 psig
Outside diameter OD = 30″ length = 45.6″
Outside surface area = 32.7 ft^2
Volume = 16.1 ft^3 = 456 L
Empty weight = 340 lb
Note: 1000# refers to 1000 lb water capacity.

The internal thermocouple (temperature) data from each experiment is plotted in Figure 5.8 below:

Solution

1. Derive the lumped parameter regression equation from Newton's law of cooling (assuming no reaction).

   The change in temperature as a function of time assuming a lumped parameter approach is described by an energy balance (with no reaction):

   Rate of heat change in the cylinder = rate of heat change to the surroundings

$$m_{\text{liquid}} Cp_{\text{liquid}} \frac{dT}{dt} = h_o A(T(t) - T_{\text{amb}}) \quad (5.6)$$

where

m_{liquid} is the mass of the liquid in cylinder
Cp_{liquid} is the specific heat of the liquid
h_o is the overall convective heat transfer coefficient for the cylinder
A is surface area for heat exchange of the cylinder.

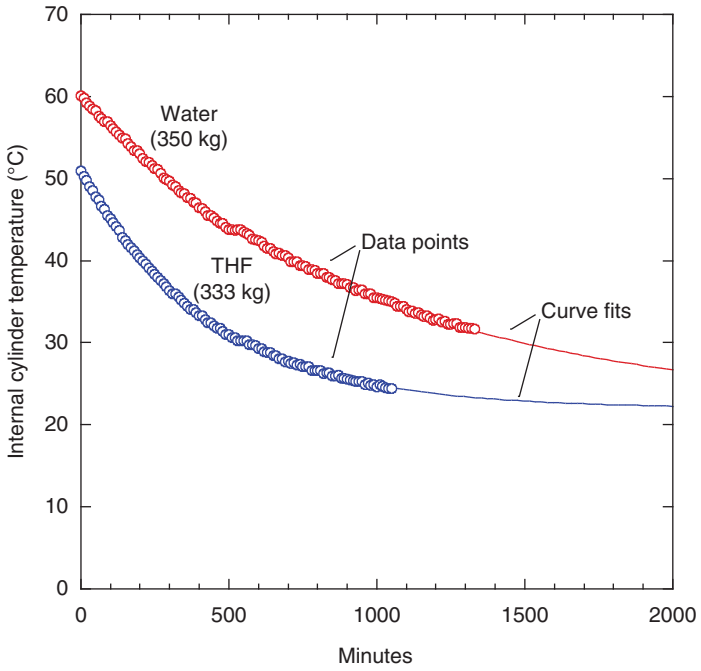

Water cooling curve

$y = 22 + m_2 \times \exp(-m_3 \times m_0)$		
Water	Value	Error
m_2	37.919	0.056 659
m_3	0.001 043 6	2.958 8e-6
Chisq	7.950 2	NA
R	0.999 55	NA

THF cooling curve

$y = 22 + m_2 \times \exp(-m_3 \times m_0)$		
THF	Value	Error
m_2	29.082	0.040 717
m_3	0.002 325 3	4.985e-6
Chisq	1.812 5	NA
R	0.999 84	NA

FIGURE 5.8 Cooling curve profiles for two separate experiments – cooling of 400 L cylinder. Ambient temperature is 22 °C. The points are experimental, and the line through the data is a regression model. The fitted parameters for the regression are shown inset as m_2 and m_3 where m_0 is time (minutes).

Note that the surface area, A, can be defined as the total surface area of the cylinder or wetted surface area based on the fill volume as long as it is used consistently.

By integrating Eq. (5.6), rearrangement, and solving for $T(t)$:

$$T(t) = \text{Tambient} + (T_i - T_{amb})\exp\left(-\frac{h_o A}{m_{liquid} Cp_{liquid}} t\right) \quad (5.7)$$

where

T_{amb} is the ambient temperature

T_i is the initial temperature.

The parameters in Eq. (5.7) were regressed shown as inset in Figure 5.8.

Notice that the term h_oA/mCp has units of (1/time), and thus the reciprocal mCp/h_oA has units of time and can be considered a thermal time constant for the vessel. This constant characterizes the temperature dynamics of the vessel:

$$\tau = \left(\frac{m_{THF} Cp_{THF}}{h_o A}\right) \equiv \text{units of time}$$

The half-life $t_{1/2}$ for cooling can be defined as

$$t_{1/2} = \ln 2 \cdot \tau = 0.693\tau$$

2. From the regression fits (Eqs. 5.3 and 5.4), the individual cooling curves were described as:
   - Cooling curve for 350 kg of water in 400 L cylinder:

$$T(t) = 22^\circ\text{C} + 37.919\exp(-0.001\ 043\ 6t)$$

   - Cooling curve for 333 kg of THF in 400 L cylinder:

$$T(t) = 22^\circ\text{C} + 29.082\exp(-0.002\,325\,3t)$$

where t is in minutes. From the regression equations, we find that the thermal time constants for THF and water are 7.2 and 16 hours, respectively:

$$\tau_{THF} = \left(\frac{m_{THF} Cp_{THF}}{h_o A}\right) = \frac{1}{0.002\ 325\ 3\ \text{minutes}^{-1}} = 430\ \text{minutes} = 7.2\ \text{hours}$$

$$t_{1/2,THF} = 0.693 \times 7.2\,\text{hours} = 5\,\text{hours}$$

$$\tau_{water} = \left(\frac{m_{water} Cp_{water}}{h_o A}\right) = \frac{1}{0.001\ 043\ 6\ \text{minutes}^{-1}} = 958\ \text{minutes} = 16\ \text{hours}$$

$$t_{1/2,water} = 0.693 \times 16\,\text{hours} = 11\,\text{hours}$$

and so the thermal half-life constants for cooling are 5 and 11 hours for THF and water, respectively. Given the much higher heat capacity of water compared with THF, it takes longer to cool the tank of water for a similar mass.

Knowing the mass and heat capacity used in the cooling experiments, we can solve for the individual heat transfer coefficients, h_oA

$$h_oA = mCp/\tau$$

- Water:

$$h_oA = \frac{350\ \text{kg} \times 4180\ \text{J/kgK}}{958\ \text{minutes}}\left(\frac{\text{minutes}}{60\ \text{seconds}}\right) = 25.45\ \text{W/K}$$

- THF:

$$h_oA = \frac{333\ \text{kg} \times 1765\ \text{J/kgK}}{430\ \text{minutes}}\left(\frac{\text{minutes}}{60\ \text{seconds}}\right) = 22.8\ \text{W/K}$$

For simplicity if A is assumed to be the outside surface area (32.7 ft^2 = 3.04 m^2) of the tank, then the individual heat transfer coefficient, h_o, can be calculated:

$$\text{Water}: h_o = hA/A = (25.45\,\text{W/K})/3.04\,\text{m}^2 = 8.4\,\text{W/m}^2\text{K}$$

$$\text{THF}: h_o = hA/A = (22.8\,\text{W/K})/3.04\,\text{m}^2 = 7.5\,\text{W/m}^2\text{K}$$

Using a per mass basis (of liquid) eliminates the uncertainty in the area term:

$$\text{Water}: h_oA/m = 25.46\,\text{W/K} \times (1/350\,\text{kg of H}_2\text{O}) \times 1000\,\text{mW/W} = 72.7\,\text{mW/kgK water}$$

$$\text{THF}: h_oA/m = 22.8\,\text{W/K} \times (1/333\,\text{kg of THF}) \times 1000\,\text{mW/W} = 68.5\,\text{mW/kgK THF}$$

These data show good consistency for two separate cooling experiments for two different liquids with dramatically different specific heats, both resulting in an outside convective heat transfer coefficient of approximately 8 W/m^2K or 70 mW/kgK for a 400 L cylinder. Table 5.1 summarizes the calculated time constants.

3. Calculate the PHI factor for the 400 L cylinder containing 350 kg of THF:
   - Assume a specific heat of carbon steel of 0.47 J/(g·°C).
   - Assume a specific heat for THF: 1765 J/(kg·K).
   - Assume mass of empty cylinder: 340 lb or 154 kg.

Solution

$$Ø = 1 + \frac{(mCp)_{\text{tank}}}{(mCp)_{\text{THF}}}$$

$$\phi = 1 + \frac{(154\,\text{kg})\left(0.473\,\frac{\text{kJ}}{\text{kg·K}}\right)}{(350\,\text{kg})\left(1.765\,\frac{\text{kJ}}{\text{kg·K}}\right)} = 1 + \frac{72.84\,\frac{\text{kJ}}{\text{K}}}{617.8\,\frac{\text{kJ}}{\text{K}}} = 1.12$$

SADT

The SADT of a material depends on the reactivity of the material, its packaging configuration, and the heat loss characteristics of that packaging. In the case of BTHF, the packaging is the particular size cylinder and the surface area to volume for heat transfer that influences the heat loss characteristics. The SADT value is important for characterizing self-reactive chemicals and establishing whether the material requires refrigeration for storage and shipping. UN transportation requirements, for example, specify that a material to be shipped must be stable at 55 °C for 7 days, while US DOT regulations require stability at 130 °F (54.4 °C) for the duration of the shipment, which could potentially be 1 week to 6 months [7].

The SADT can be determined by several different methods, one of which is via the classic Semenov plot. This is done by plotting the heat generation rate and heat loss rate as a function of temperature. The rate of heat loss of the container depends on the difference between the internal cylinder temperature and the ambient temperature (i.e. $T_r - T_{amb}$). The Semenov diagram is one approach used to estimate the critical ambient temperature where the heat generation rate exceeds the heat loss. This critical temperature is the SADT, typically rounded up to the nearest 5 °C interval.

TABLE 5.1 Heat Transfer/Parameters Obtained for the Cooling Curves (Shown in Figure 5.8)

Test	Mass Used (kg)	Overall A (m^2)	mCp/hA (hr)	Half-Life $t_{1/2}$ (h)	h_oA (W/K)	h_oA/mass (mW/kgK)	h_o (W/m^2K)
Water	350	3.04	16	11	25.46	72.7	8.4
THF	333	3.04	7.2	5	22.8	68.5	7.5
Average					*24.1*	*70.6*	*8.0*

Parameter h_o is the heat transfer coefficient between the tank and ambient air.

EXAMPLE PROBLEM 5.4

1. Construct a Semenov diagram based on the ARC data shown in Figure 5.4 and the cooling curve data for THF from Table 5.1. Assume the tank contains 350 kg of BTHF in the packaging configuration of a 400 L cylinder. Assume a PHI correction of 2.4 for the ARC data and a specific heat (*Cp*) of 1740 J/kgK for the BTHF sample.
2. Estimate the SADT (i.e. the critical ambient temperature).
3. Estimate the temperature of no return (TNR) (i.e. temperature inside the cylinder).

Solution

1. To construct the Semenov diagram, first start with the heat generation rate:

   The ARC data shown in Figure 5.4 was used to regress parameters from a plot of self-heat rate vs. $1/T$ where T is in Kelvin:

   From ARC data (Figure 5.4)

$$\text{Self-heat rate}\left(^{\circ}\text{C/min}\right) = \frac{dT}{dt} = 3.2965 \times 10^{12}\exp\left(-10446\left(\frac{1}{(T^{\circ}\text{C}+273.15)}\right)\right)$$

To convert the self-heat rate data from the ARC to heat generation rate, we need to correct for phi and convert the units to watts per liter:

$$\text{Heat Generation Rate (HGR)} = \text{Ø}\cdot\rho\cdot Cp\frac{dT}{dt} = 2.4\times 1740\frac{\text{J}}{\text{kg}\cdot\text{K}}\cdot\frac{0.89\ \text{kg}}{\text{L}}\left(3.2965\times 10^{12}\exp\left(-10446\left(\frac{1}{T}\right)\right)\frac{\text{K}}{\text{min}}\right)\cdot\left(\frac{\text{min}}{60\ \text{s}}\right) \equiv \text{W/L}$$

You should recognize that 10 446 K = E_a/R (E_a = 86.8 kJ/mol = 20.7 kcal/mol) where E_a is the activation energy and R is the gas constant.

The heat loss rate for the 400 L cylinder containing 350 kg of BTHF inside the storage cylinder and using h_oA obtained from Table 5.1:

$$Q_{\text{Heat loss}} = h_oA(T-T_{\text{amb}}) \equiv W$$

$$\text{Heat loss rate} = Q_{\text{Heat loss}}\cdot\frac{1}{\text{mass}}\cdot\rho \equiv \text{W/L}$$

$$= \frac{22.8\,W}{\text{K}}\frac{1}{350\,\text{kg}}\cdot\frac{0.89\,\text{kg}}{\text{L}}(T-T_{\text{amb}}) = 0.058\frac{\text{W/K}}{\text{L}}(T-T_{\text{amb}}) \equiv \text{W/L}$$

Next, using a spreadsheet, generate points for the heat generation rate and heat loss functions (shaded in red indicate when HGR exceeds heat loss).

Temp (°C)	Heat Gen. Rate (W/L)	Heat Loss T_{amb}=32 °C (W/L)	Heat Loss T_{amb}=29 °C (W/L)	Heat Loss T_{amb}=28 °C (W/L)	Heat Loss T_{amb}=27 °C (W/L)
25	0.124	–0.406	–0.232	–0.174	–0.116
30	0.221	–0.116	0.058	0.116	0.174
35	0.387	0.174	0.348	0.406	0.464
40	0.665	0.464	0.638	0.696	0.754
43	0.913	0.638	0.812	0.870	0.928
45	1.124	0.754	0.928	0.986	1.044
50	1.867	1.044	1.218	1.276	1.334
55	3.056	1.334	1.508	1.566	1.624
60	4.928	1.624	1.798	1.856	1.914

Keep in mind that the x-axis of the Semenov plot is the internal temperature of the cylinder. So when the internal temperature is exactly equal to the outside temperature, there is no heat exchange taking place. So for the heat loss curve, plot lines at various ambient temperatures. For example, at T_{ambient} = 29 °C starts at 29 °C on the x-axis where y = 0 and with a slope of 0.058 (W/K)/L as shown in Figure 5.9. Plot the heat generation and heat loss equations between 25 and 50 °C using T_{ambient} of 29 °C. As shown in Figure 5.9, the straight heat loss curve intersects the heat generation curve very close to a single point. The point of

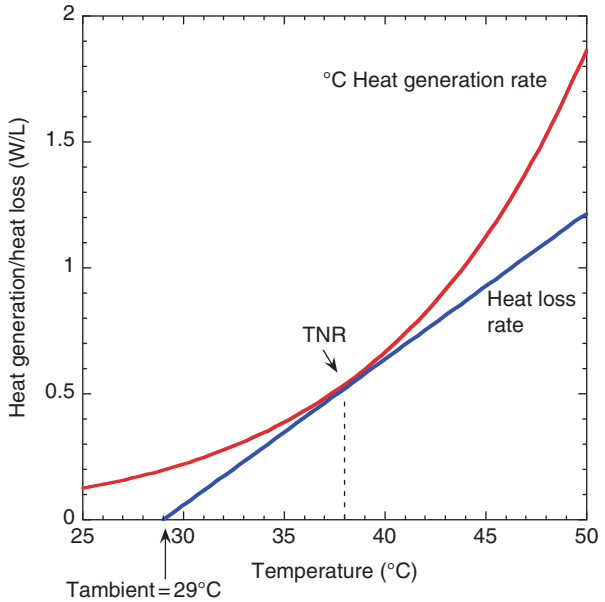

FIGURE 5.9 Semenov plot to determine SADT for aged BTHF. Red curve is the heat generation based on ARC data. The blue curve is the heat loss from the 400 L cylinder when the ambient temperature is 29 °C. The intersection at the tangent is the critical point or temperature of no return (TNR).

intersection is the critical point where heat generation and heat loss are equal and is considered unstable because a slight shift will cause the heat generation to exceed heat loss, leading to a thermal runaway.

2. The SADT is the ambient temperature at which this intersection is found, in this case near 29 °C. Solve in Excel or trial and error at 28.8 °C.
3. From the same graph, the TNR inside the cylinder is found near 38 °C. Above this temperature thermal equilibrium is no longer possible, resulting in thermal runaway. Note that T_{NR} can also be calculated from

$$\frac{E_a}{R} = \frac{T_{NR}^2}{(T_{NR} - T_{ambient})} = 10\,446\,\text{K}$$

where E_a/R was obtained from the ARC data. (Note: keeping all temperatures in Kelvin, and setting $T_{ambient} = 29$ °C, the T_{NR} is found to be 38.285 K.)

From the initial ARC tests of the aged BTHF, we showed that the TD24 was approximately 27 °C. Thus, under purely *adiabatic* (no heat loss) conditions, this composition of BTHF can self-heat and have a runaway reaction from 27 °C (81 °F) such that the maximum rate will be reached in 24 hours. By constructing the Semenov plot, we added a new constraint of heat loss occurring between the tank and the surrounding air. With the heat loss considered, the data showed the heat generation exceeds the rate of heat loss when the outside air temperature reaches 29 °C (84 °F). The explosion occurred on 25 June where the peak temperature the previous day was (29 °C) (84 °F) by 4:00 p.m., 16 hours prior to the explosion. As the ambient temperatures increased, the internal tank temperature was even warmer than 29 °C due to the internal self-heating, and after several hours (due to the time constant for heating/cooling), it was likely closer to 38 °C inside the tank. At this critical TNR point, the internal temperature can keep rising even if the ambient temperature starts to cool (e.g. evening/nighttime).

What is not immediately evident is how long must the peak ambient temperatures need to be sustained for the runaway reaction to occur. The peak daytime temperature was maintained for a short time before it began decreasing again. This required additional kinetic analysis, which will be discussed in more detail in a subsequent section. However, what we can say from the Semenov analysis is that the SADT was determined to be surprisingly low (below 30 °C) for aged BTHF, certainly well below the limits necessary to ship without refrigeration per US DOT transportation guidelines for self-reactive materials.

5.7 THERMAL STABILITY OF FRESH 2M BORANE–THF

Up to now we have discussed ARC data and analysis for "aged BTHF" recovered from the surviving cylinders where the potency of BTHF was approximately 1.3 M (originally ~1.9 M) BTHF and the remaining active hydride was approximately 1.4 M. After the incident, the manufacturer provided samples from the original lot that had been retained at their site under refrigeration. Those retained samples were also studied by ARC.

ARC testing of the retained refrigerated (fresh) 2M BTHF, from the same originating lot, using the standard HWS method is shown in Figure 5.10. The effect of stabilizer is clearly

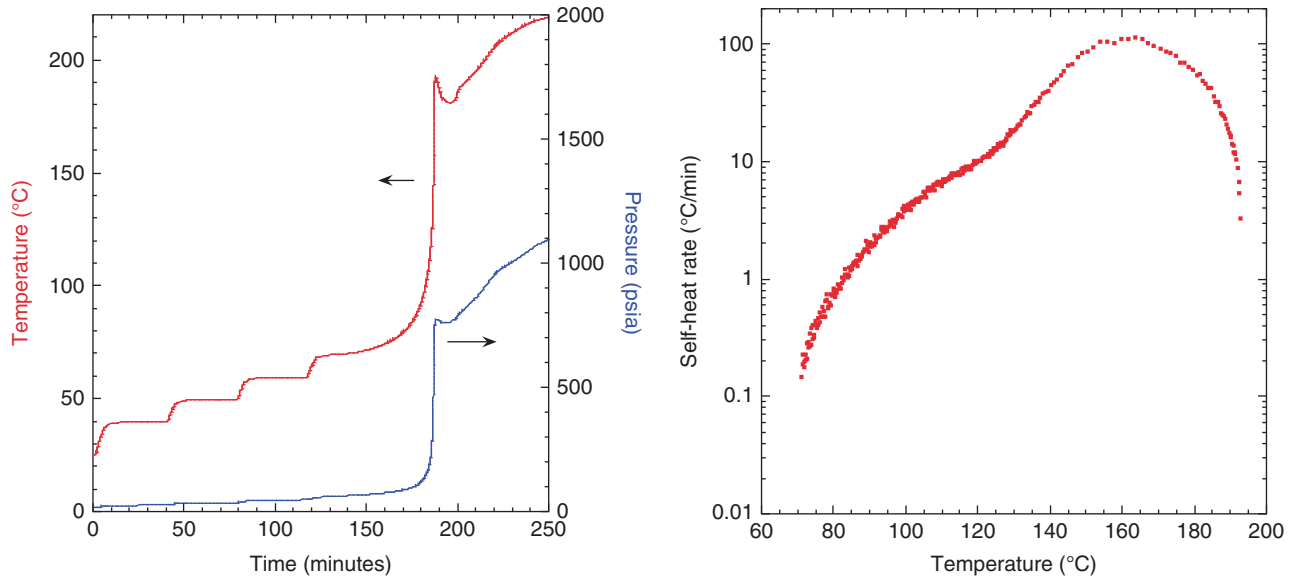

FIGURE 5.10 1.9 M BTHF G24890 ARC data (standard heat-wait-search method (HWS) in a titanium test cell; phi = 2.4). Temperature vs. time (left) and self-heat rate (SHR) (right) vs. time. The effect of stabilizer in refrigerated BTHF is apparent by the delayed onset temperature and curvature in SHR starting at 70 °C.

evident as the onset temperature is delayed as compared with the aged sample (70 °C vs. 50 °C). In the standard HWS method, the exotherm criterion is met when the self-heating rate exceeds 0.02 °C/min. And there is a significant difference in the self-heat profiles between the refrigerated and aged samples. The adiabatic temperature rise when corrected for PHI was 288 °C (120 × 2.4) with pressure rise exceeding 1000 psi.

The role of the stabilizer is to slow the ring-opening decomposition kinetics, but as the stabilizer's effectiveness diminishes, the rate of decomposition increases. This explains the *observed* pseudo-autocatalytic behavior in the ARC data where the apparent change in mechanism is due to the loss of effectiveness of the stabilizer. This was not observed in the aged samples because the effect of stabilizer was fully depleted and effectively absent.

To study the effect of aging, isothermal aging studies were performed in the ARC from 40 °C, as well as 30 °C, initial temperatures. In all cases, the BTHF samples were observed to self-heat from the lowest test temperatures of 30 °C in the ARC. For refrigerated 2M BTHF, several days at 30 °C were required to deplete the stabilizer. Refrigerated BTHF with stabilizer has a longer TMR than aged samples. The TMR depends on the remaining level of stabilization, which depends on the temperature–time history of the sample. The dramatic difference between the refrigerated and aged samples is reflected in the iso-age ARC study shown in Figure 5.11.

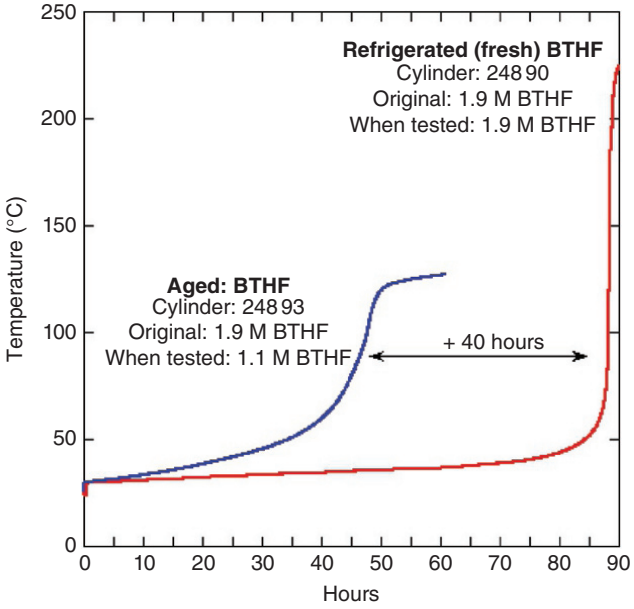

FIGURE 5.11 Iso-age ARC results of BTHF samples. Aged low potency (1.1 M) BTHF (blue curve) shows immediate self-heating from 30 °C. Refrigerated 2M BTHF (1.9 M) requires 87 hours (3.5 days) before runaway (red curve). These data illustrate the effect of loss of stabilization after aging.

The aged sample shows no stabilizer effect remaining, while the refrigerated material required 3.5 days when starting the experiment at 30 °C before thermal runaway.

We also performed accelerated aging studies on refrigerated BTHF. In this case we took small samples of previously refrigerated BTHF and held them isothermally at 50 °C for 3 and 7 hours, respectively, and compared them without any accelerated aging. The results are shown in Figure 5.12.

The stabilization effect of the sodium borohydride on the decomposition complicates the thermal analysis. For example, if we only looked at the HWS profile for refrigerated 2M BTHF, it would appear to have much higher stability (onset at 70 °C). Further with the apparent pseudocatalytic behavior due to the stabilizer, we cannot reliably extrapolate the self-heat curve to lower temperatures. To adequately address the influence of stabilizer, iso-aging studies were required as was shown in Figure 5.12.

What we can conclude from the refrigerated BTHF thermal testing is that the TMR for thermal decomposition depends on the level of stabilizer effectiveness, which in turn depends on the time–temperature history of the samples.

All 2M BTHF samples (whether refrigerated or aged) were found to self-heat in less than 4 days from our lowest starting ARC temperature of 30 °C.

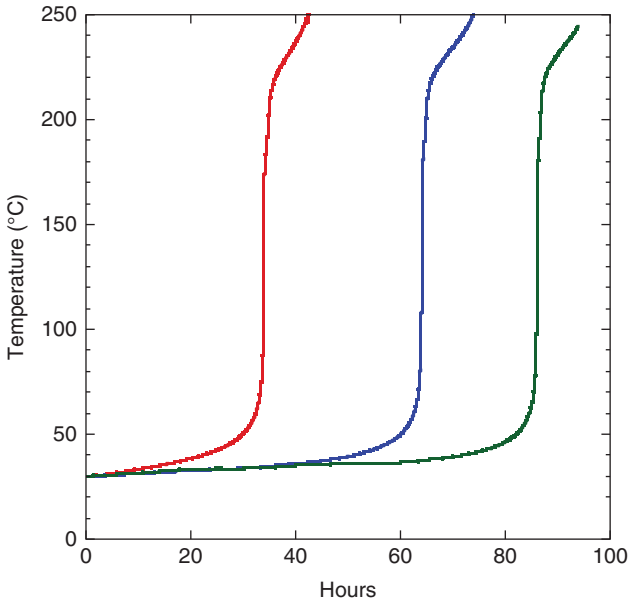

FIGURE 5.12 Effect of accelerated "age" time on TMR. Leftmost curve, the sample was pre-aged at 50 °C for 7 hours. This aging had the effect of depleting the stabilizer, resulting in a TMR of approximately 32 hours. Similarly a sample "aged" at 50 °C for only 3 hours had a TMR of approximately 62 hours (middle curve). No pre-aging sample showed a TMR of over 80 hours (rightmost curve). Regardless of the "aging" time, all samples eventually self-heated from 30 °C.

5.8 KINETICS OF DECOMPOSITION

It is known that BTHF solutions slowly degrade to tributyl borate. In a patent granted to the manufacturers of BTHF, the authors wrote that the "exact mechanism of thermal decomposition has not been determined. The overall decomposition does not follow first- or second-order kinetics. Several possible mechanistic routes can be envisioned" (Burkhardt and Corella [4]).

As part of the incident investigation, a kinetic model was developed to help understand the kinetics of decomposition, including the role of the stabilizer and its depletion with time and temperature. Temporal compositional data were collected at several temperatures, and plausible mechanisms were tested by regressing their respective kinetic models to the actual data. A good fit of the model does not necessarily prove the mechanism, but it demonstrates that the proposed mechanism is at least consistent with kinetic data within the range of temperatures and compositions tested.

One plausible mechanism that was highly consistent with the kinetic data is shown in Scheme 5.2:

The kinetic profiles based on isothermal NMR data are shown in Figure 5.13. These data were obtained by placing refrigerated (fresh) 2M BTHF in quartz NMR tubes and holding them at a constant temperature in temperature baths for days. NMR scans were taken periodically to obtain the temporal compositions.

Notice the induction times, especially for the lower temperatures, where the effect of the stabilizer is evident. After this initial induction time, the stabilizer effectiveness essentially becomes depleted, and the decomposition kinetics transitions to what appears to be unstabilized kinetics. The data points were obtained from ^{11}BNMR measurements and converted to molar concentrations. The kinetics (line fits through the data) were mathematically described by the respective differential rate equations shown in Schemes 5.3 and 5.4.

A kinetic inhibition function was used to describe the level of stabilizer [S] present where [S] has a value between 0 and 1. Given [S], the conversion (or loss) of stabilizer is defined as $X_s = 1 - [S]$. For example, new BTHF is fully stabilized, so $S = 1$ and the loss of stabilizer $X_s = 0$, while fully aged BTHF has effectively no stabilizer, so $S = 0$ and $X_s = 1$. The rate at which the stabilizer is depleted is temperature dependent and is well captured by the model. This is evident by the line through the data points of Figure 5.13, which is based on the regression fit of the kinetic model.

When the stabilizer is new, the first reaction (A → M) is fully inhibited so mathematically k_1 is inhibited by the initial level of stabilizer where $S = 1$ and the "loss" of stabilizer $X_s = 0$. As the stabilizer degrades with time and temperature [S] tends toward 0 and X_s =1. So to accurately describe the effect of stabilizer in the model, we multiply k_1 by X_s to slow the rate of decomposition. As the stabilizer is depleted, X_s approaches 1 (i.e. unstabilized), having the effect of accelerating the rate, so the detailed kinetic model describes both stabilized and unstabilized decompositions of BTHF. The detailed model is shown in Scheme 5.4 where Eqs. (5.1)–(5.6) describe the compositional changes in the liquid phase.

Each data set (Figure 5.13) was regressed using the detailed model shown in Scheme 5.4. Since [M] is never observed, suggesting k_2 must be fast, we assigned k_2 to be

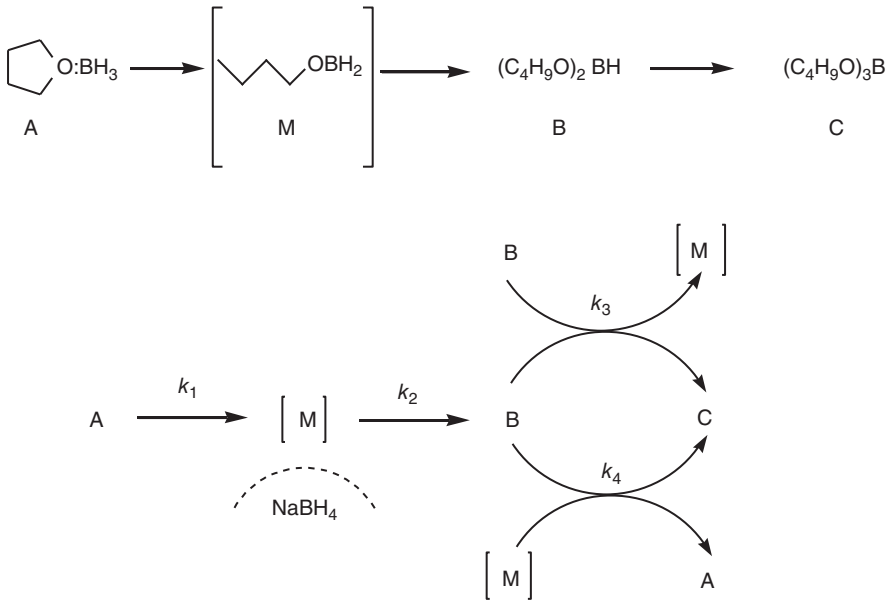

SCHEME 5.2 Top: Overall decomposition scheme. Bottom: Proposed mechanistic network where mono M is inhibited by the presence of active inhibitor or stabilizer (sodium borohydride). B can react in bimolecularly with [M] or another B. For simplicity, these reactions are considered irreversible.

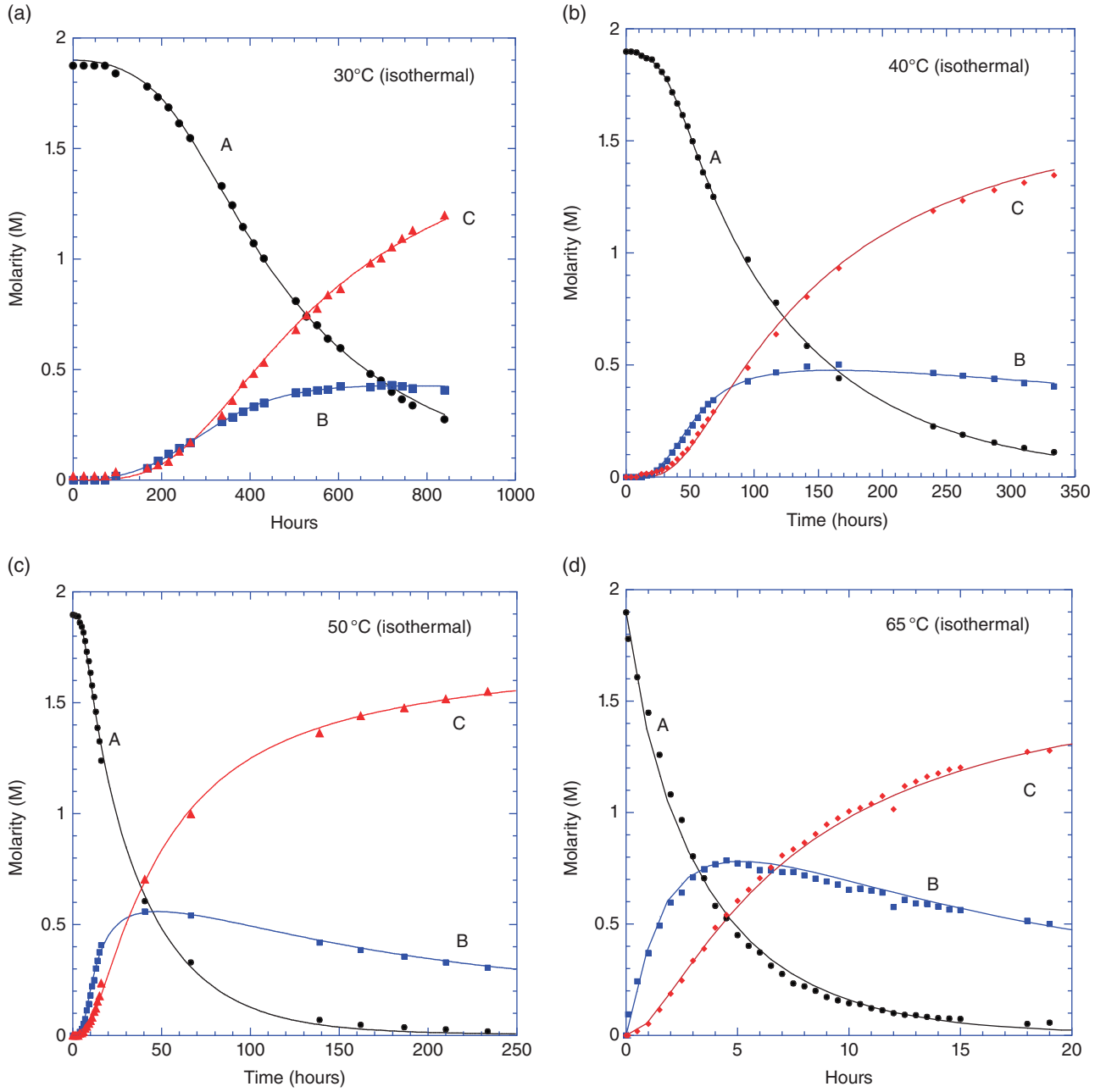

FIGURE 5.13 Kinetic profiles for ring-opening decomposition of BTHF at (a) 30 °C, (b) 40 °C, (c) 50 °C, and (d) 65 °C, where A is BTHF, B is dibutoxyborane, and C is tributylborate. The initial concentration of BTHF was 1.9M. Points were based on concentrations from boron ^{11}NMR and the curve fit lines were regressed via kinetic model in Scheme 5.4. The concentration data are also tabulated in the Appendix 5.A.

$$\frac{dA}{dt} = -k_1[A] + k_4[M][B]$$

$$\frac{dM}{dt} = k_1[A] - k_2[M] + k_3[B]^2 - k_4[M][B]$$

$$\frac{dB}{dt} = k_2[M] - 2k_3[B]^2 - k_4[M][B]$$

$$\frac{dC}{dt} = k_3[B]^2 + k_4[M][B]$$

$$\frac{dS}{dt} = -k_s \times [S] \times (1.037\,19 - S)$$

SCHEME 5.3 General kinetic model for the thermal decomposition of 2 M BTHF stabilized with 0.005 M sodium borohydride and where the initial conditions: A = 1.9 M, B = 0, C = 0, M = 0, S = 1.

$$\frac{dS}{dt} = -k_s\, S\, (1.037\,19 - S)$$

$$X_s = 1 - S$$

$$\frac{d[A]}{dt} = -k_1[A]X_s + k_4[M][B]$$

$$\frac{d[M]}{dt} = k_1[A]X_s - k_2[M] + k_3[B][B] - k_4[M][B]$$

$$\text{but } k_2 \gg k_1 \text{ so } k_2 \approx 63k_1X_s$$

$$\frac{d[B]}{dt} = k_2[M] - 2k_3[B][B] - k_4[M][B]$$

$$\frac{d[C]}{dt} = k_3[B][B] + k_4[M][B]$$

SCHEME 5.4 Detailed kinetics used for parameter estimation and fitting of the data shown in Figure 5.13.

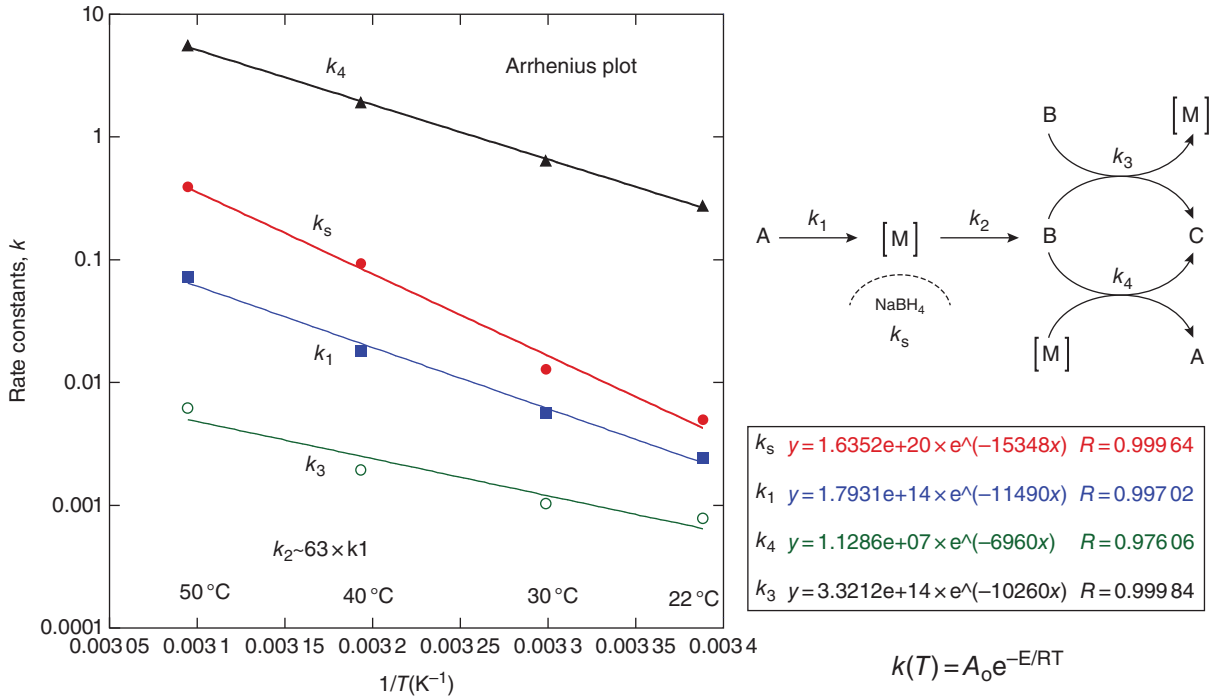

FIGURE 5.14 Arrhenius plot based on the best fits from each of the isothermal kinetic data sets.

proportional to k_1. After regression analysis at all temperatures, we determined $k_2 \approx 63k_1$. After each set of concentration data was regressed at each temperature, an Arrhenius plot provided activation parameters as shown in Figure 5.14. The highest activation energy was for the loss of stabilization, k_s at 30.5 kcal/mol. And the larger the activation energy, the more sensitive the reaction rate is to temperature. It follows that the loss of stabilization is the most sensitive to temperature where, for example, BTHF is stable for months below 0 °C, while only a few days at 30 °C.

The parameter estimates were obtained from each set of kinetic data. k_2 is considered much faster than k_1 and was thus fixed at $63 \times k_1$.

T(°C)	$1/T$ (K)	k_s (h^{-1})	k_1 (h^{-1})	k_3 ($h^{-1}M^{-1}$)	k_4 ($h^{-1}M^{-1}$)
22	0.003 388 1	0.004 982	0.002 472 0	0.000 784 6	0.275 0
30	0.003 298 7	0.012 854	0.005 709 2	0.001 038 0	0.641 7
40	0.003 193 4	0.093 740	0.018 045 0	0.001 940 3	1.921 3
50	0.003 094 5	0.392 750	0.073 130 0	0.006 210 0	5.547 4

In order to couple the reaction kinetics to the storage conditions, the model was extended to include the thermochemistry and energy balances. Equation (5.8) is the basic energy balance for the cylinder, which describes how the temperature changes, depending in the rate of heat generation from BTHF decomposition and the rate of heat removed from the storage container. Equation (5.9) describes the rate of heat transferred through the wall of the tank or storage vessel. Equation (5.10) describes the rate of heat generation from the BTHF decomposition pathway where

$H_1 = -35.4$ kcal/mol
$H_2 = -39.4$ kcal/mol
$H_3 = -5.8$ kcal/mol
$H_4 = -9.8$ kcal/mol

The overall heat of reaction was measured by CRC90 calorimeter to be approximately $\Delta H = -120$ kcal/mol of BTHF. This was consistent with thermodynamic calculations based on heats of formation of BTHF and tributyl borate, resulting in a calculated $\Delta H - 126$ kcal/mol.

Energy balance:

$$\frac{dT}{dt} = \frac{Q_{\text{generation}} - Q_{\text{loss}}}{Cp \cdot \rho} \tag{5.8}$$

where

$$Q_{\text{loss}} = \frac{U \cdot A \cdot (T_r - T_{\text{ambient}})}{V} \tag{5.9}$$

and where

$$Q_{\text{generation}} = k_1[\text{A}]X_s\Delta H_1 + k_2[\text{M}]\Delta H_2 + k_3[\text{B}][\text{B}]\Delta H_3 + k_4[\text{M}][\text{B}]\Delta H_4 \quad (5.10)$$

The model parameters:

$[\text{A}]_{\text{initial}} = 1.9$ M

$[\text{B}]_{\text{initial}} = [\text{C}]_{\text{initial}} = [\text{M}]_{\text{initial}} = 0$

$S_{\text{initial}} = 1$

$\rho = 0.87$ kg/L

$Cp = 1775$ J/(kg·K)

UA = 21.9 W/K (heat loss of the cylinder)

$V = 400$ L

Initial temperature, $T_r = T_{\text{initial}}$, (initial temperature depends on the model scenario)

Heats of reaction:

Overall heat of reaction: $\Delta H_{\text{rxn}} = -120$ kcal/mol $= -502.1$ kJ/mol

$\Delta H_1 = -35.4$ kcal/mol

$\Delta H_2 = -39.4$ kcal/mol

$\Delta H_3 = -5.8$ kcal/mol

$\Delta H_4 = -9.8$ kcal/mol

Note that

$\Delta H_3 = \Delta H_{\text{rxn}} - \Delta H_1 - 2\Delta H_2$

$\Delta H_4 = \Delta H_{\text{rxn}} - 2\Delta H_1 - \Delta H_2$

Arrhenius parameters from (Figure 5.14):

$k_s = 1.635 \times 10^{20}\exp(-15\,348/(T_r + 273.15)) \equiv \text{hour}^{-1}$ ($E_s = 30.5$ kcal/mol)

$k_1 = 1.79 \times 10^{14}\exp(-11\,500/(T_r + 273.15)) \equiv \text{hour}^{-1}$ ($E_1 = 22.9$ kcal/mol)

$k_3 = 1.13 \times 10^{7}\exp(-6\,960/(T_r + 273.15)) \equiv \text{hour}^{-1}$ ($E_3 = 13.8$ kcal/mol)

$k_5 = 3.32 \times 10^{14}\exp(-10\,300/(T_r + 273.15)) \equiv \text{hour}^{-1}$ ($E_5 = 20.5$ kcal/mol)

The model (based on Scientist/Micromath software) enabled dynamic temperature and composition simulations. With this working model, we were able to simulate composition and temperature of the 400 L cylinder based on different storage conditions. For example, in Figure 5.15 we calculate the internal temperature profiles for various ambient temperatures. The simulation shown in Figure 5.15 assumes the cylinder is removed from a cold storage of 2.5 °C and held at constant ambient temperature. We show that sustained ambient temperature of 22 °C for the 400 L cylinder would likely result in thermal runaway starting with new 2M BTHF, requiring about 1 month to destabilize and for thermal runaway to occur.

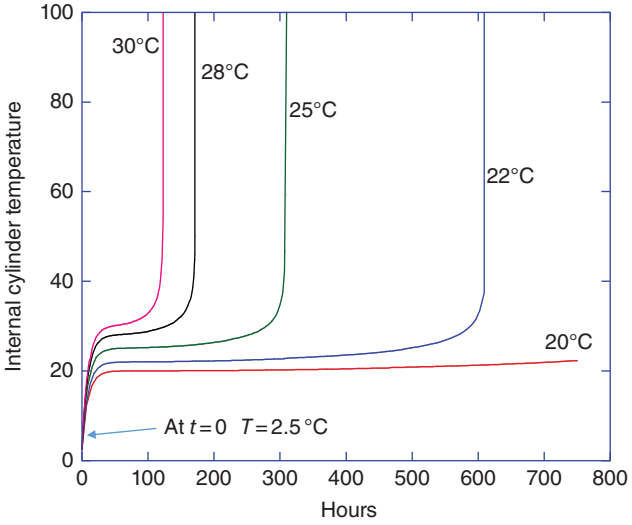

FIGURE 5.15 Simulations starting with refrigerated (fresh) 1.9 M BTHF in 400 L cylinder initially at 2.5 °C and placed at various ambient temperatures. Each curve is a separate ambient temperature. The model is showing that the cylinder containing 350 kg of BTHF will self-heat (thermal runaway) at temperatures as low as 22 °C if given sufficient time (25 days) as compared with approximately 5 days at 30 °C.

In a similar way we simulate the effect of initial concentration in Figure 5.16. It shows that concentrations above 1 M are most susceptible to thermal runaway in this size cylinder. We took the analysis a step further by modeling the nonlinear ambient temperature profile for the full duration of storage in the flammable materials warehouse as shown in Figure 5.17.

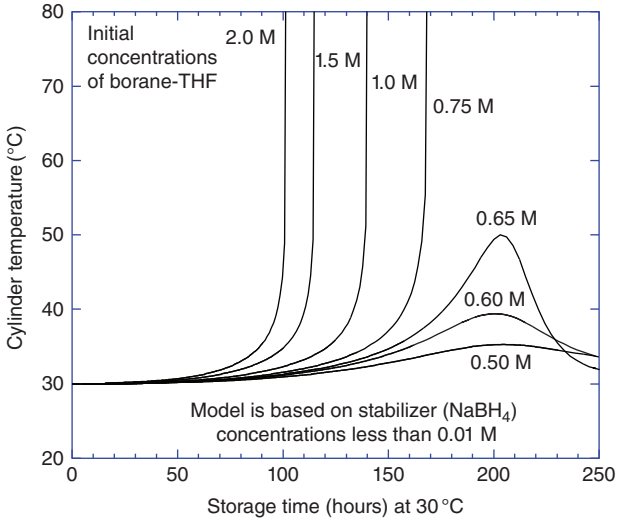

FIGURE 5.16 Simulations of different starting concentrations of new BTHF in 400 L cylinder stored at 30 °C. Each curve assumes a different initial concentration of BTHF.

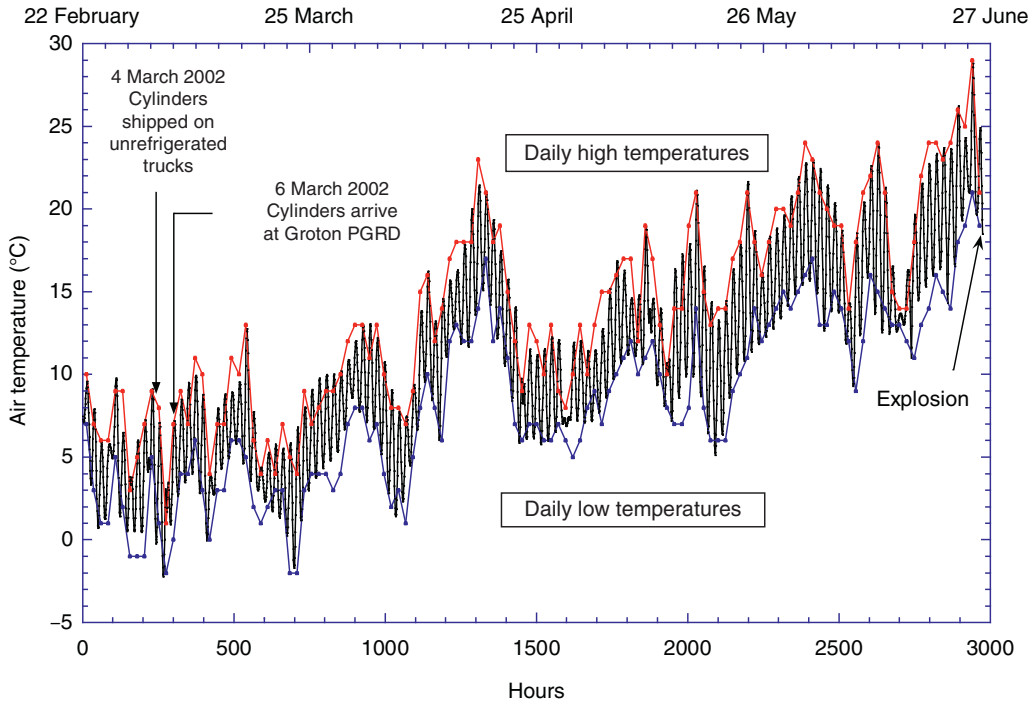

FIGURE 5.17 Ambient temperature history based on chart recorder in the flammable materials warehouse where the cylinders were stored. The high points are the daily high temperatures. The low points are the daily low temperatures. The black line is the numerical function describing the temperature history as a sinusoidal $T_{\text{ambient}} = f(\sin(x))$, which was used in the kinetic model to describe the external temperature.

Each daytime high and low temperature was fit to a sinusoidal temperature function to approximate the general daily temperature trend. Figure 5.17 shows an accurate ambient temperature history that the six cylinders were exposed to during the duration of storage in B196 warehouse. By applying this nonlinear ambient temperature profile to the thermokinetic model, the internal cylinder temperature can be modeled as shown in Figures 5.18 and 5.19.

From Figure 5.18 we see the internal temperature climb during the spring months. The stabilizer has been depleted by the end of May based on the potency starting to drop (near 1.8 M). For the month of June, the BTHF cylinders are essentially unstabilized. The last five days are shown in Figure 5.19.

What we see from Figure 5.19 is the temperature oscillation is very apparent (due to the daytime heating and cooling). For 23 and 24 June, however, was the first time that the nighttime temperatures remained high (above 20 °C), pushing the internal temperature to over 25 °C. The peak temperature on June 24th, the day before the explosion, was the hottest day of the year to that date, reaching 29 °C. This appears to be where the internal temperature in the cylinder slipped past the critical TNR point consistent with the Semenov analysis. It took 16 more hours, as can be seen in Figure 5.19, for the cylinder to approach its maximum rate, and by 8:00 a.m. on 25 June, the cylinder was observed to be misshapen and smoking, moments before it exploded.

5.9 CONCLUSIONS

This case study focused on understanding the cause of a BLEVE involving a cylinder of 2M BTHF. The cause of the explosion was a thermal runaway reaction of a self-reactive material (BTHF) in a package configuration that was unable to adequately dissipate the heat-generated reaction. Upon the prolonged storage, between 6 March and 25 June 2002, especially as the temperatures became warmer, the stabilizer in the 2M BTHF eventually became depleted. As a result, the rate of the ring-opening decomposition reaction increased, leading to a corresponding drop in potency of BTHF. The rate of decomposition of BTHF is fairly slow, but the reactions are highly exothermic (~120 kcal/mol). In fact, there is enough exothermic potential to raise the temperature to approximately 600 °C based on the initial concentration of BTHF.

Further, the SADT for this packaging configuration had not been characterized before it arrived at the Pfizer

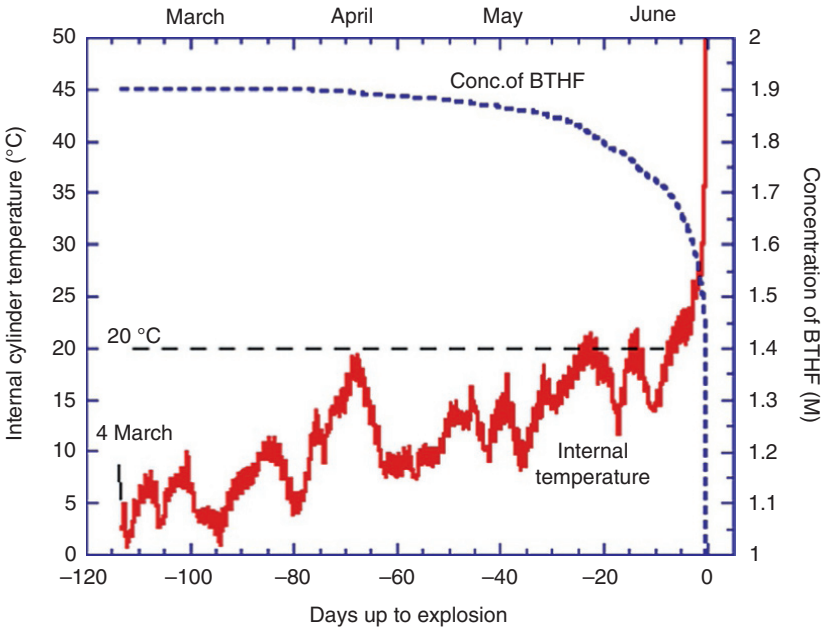

FIGURE 5.18 Simulation of the internal temperature of the exploded cylinder during its storage. Initial condition is 350 kg of 1.9 M BTHF and placed in storage. The ambient temperature history from the flammable materials warehouse was used in the simulation.

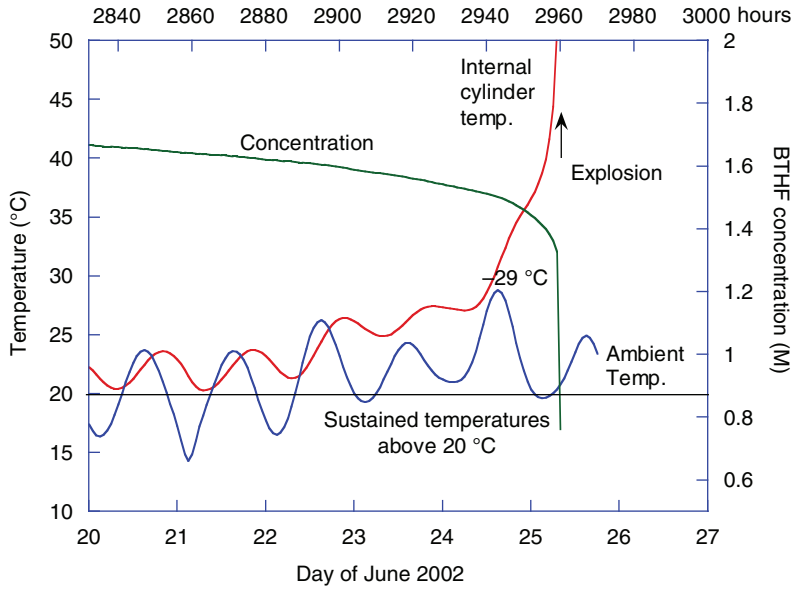

FIGURE 5.19 Simulation for the internal temperature (400 L cylinder), concentration of remaining BTHF, and ambient temperature for the five days, leading up to the explosion.

site. As part of the incident investigation, the SADT was determined to be well below 50 °C, which would have required refrigeration during transportation per DOT guidelines. The investigation also showed through ARC studies that even refrigerated, fully stabilized 2M BTHF can self-heat from the lowest test temperature of 30 °C. Performing an energy balance (Semenov plot) and using the thermal data from the aged low potency BTHF recovered from one of the surviving cylinders showed the SADT of BTHF to be 29 °C despite its lower potency.

Kinetic modeling suggests that this SADT could be even lower, when starting with new 2M BTHF and allowing it to be held at isothermal (ambient conditions) for extended periods. SADT values this low represent a serious safety concern especially considering the potential heat that can be liberated.

The investigation also showed that sodium borohydride stabilizer provides only temporary inhibitory benefit and, in fact, becomes depleted with time and temperature. Further it was shown that BTHF that is retained at room temperature will eventually behave as if it is unstabilized. Aged BTHF recovered after the incident behaved similarly to *unstabilized* laboratory-prepared BTHF of similar concentration as both exhibited very similar self-heating rates by ARC testing.

A comprehensive kinetic model was developed that was found to be consistent with extensive decomposition kinetic data over the temperature range of interest. The thermodynamics of the BTHF decomposition and thermal characteristics of the packaging configuration (400 L cylinder) were also incorporated into a complete thermokinetic model. This modeling effectively described how the internal temperature of a 400 L cylinder of BTHF responds with time and the variable and oscillating daily temperatures experienced during the three months of storage. This showed that the stabilizer became depleted and the BTHF was effectively unstabilized during the month of June 2002. The model has been provided as part of this case study.

Two important points are noteworthy regarding the ambient temperature:

1. The day before the explosion was the hottest day recorded during the entire storage time reaching 29 °C.
2. The two days preceding the explosion (23 and 24 June) represented the only window of time during the nearly 3000 hours of storage where the ambient temperatures remained above 20 °C for a duration of 48 hours. All previous days saw significantly cooler nights. It was during this 48 hours window that the internal cylinder temperature exceeded the critical point of no return.

It is also important to note that the potency of the cylinders was slowly diminishing. The kinetic model suggests that most of the decline in potency of the BTHF occurred in the month of June. In fact, the model suggests that the potency was dropping from 1.65 to 1.5 M during those few days prior to the explosion. This is also consistent with the measured potencies of the remaining cylinders. Had the cylinders been delivered a week or two later than they were, the concentrations of BTHF would have been even higher (e.g. 1.7 M) during those critically warm days of 23 to 24 June. In that case, with slightly higher potencies, and higher rates of decomposition, the slightly lower SADT's may have resulted in thermal runaway in multiple cylinders.

Self-reactive materials require thorough safety evaluations. Materials that require stabilization (added stabilizers and inhibitors) present additional complexities to fully characterize. With BTHF, the thermal stability depends on both temperature and age of the sample. Thus a single scanning experiment by DSC, ARC, or adiabatic dewar is not sufficient to adequately characterize the SADT of a stabilized self-reactive material.

Aging studies and iso-aging studies are required to assess the impact of age and temperature history on the self-heating rates and SADT. With BTHF stabilized by $NaBH_4$, the effectiveness of the stabilizer diminishes, eventually behaving as unstabilized BTHF when stored at ambient temperatures. In general for self-reactives, thorough characterization and understanding of the energy potential, self-heat rates, and effect of aging are required to properly assign SADTs and storage conditions.

ACKNOWLEDGMENTS

There were many contributors to the technical data presented in this chapter. Extensive ARC testing and analysis including the validation of phi experiments described in the appendix, David R. Bill; heat of reaction estimation and data fitting to provide sinusoidal function for ambient temperature as function of storage time, Ray Bemish; additional heat of reaction estimates, Don Knoechel; a heat of reaction measurement from CRC90, Matt Jorgensen; heat transfer (cooling curves) measurements (in various cylinders), Steve Brenek, Sandeep Kedia, and Brian Morgan; NMR analysis and studies, Andy Jensen and Linda Lohr; and additional BTHF studies, Eric Dias.

5.A BORON NMR KINETIC DATA FROM FIGURE 5.13

room temperature ≈22 °C NMR data				30 °C NMR data				40 °C NMR data				50 °C NMR data				65 °C NMR data			
hrs	BTHF	DI	TRI	hrs	BTHF	DI	TRI	hrs	BTHF	DI	TR	hrs	BTHF	DI	TR	hrs	BTHF	DI	TR
0	1.9	0	0	0	1.875	0	0.01875	0	1.8988	0	0	0	1.8971	0	0	0	1.899164	0	0
24.0	1.893688	0	0	24	1.875	0	0.01875	4	1.8978	0	0	0	1.9	0	0	0.1	1.780204	0.095063	0
48.0	1.881188	0	0.018812	48	1.875	0	0.01875	8	1.8949	0	0	1	1.9	0	0	0.5	1.608217	0.242358	0.018495
72.5	1.875	0	0.01875	72.5	1.875	0	0.01875	12	1.8801	0	0.012784	2	1.9	0	0	1	1.448723	0.370728	0.05143
96.0	1.875	0	0.01875	96	1.83871	0.018387	0.036774	16	1.8686	0.006914	0.015696	3	1.9	0.000378	0	1.5	1.258851	0.493721	0.114681
168.0	1.856678	0.018567	0.018567	168	1.779582	0.053387	0.053387	20	1.863	0.009501	0.017698	4	1.9	0.017307	0.009491	2	1.08086	0.596743	0.188178
192.0	1.856678	0.018567	0.018567	192	1.730944	0.086547	0.069238	24	1.835	0.02991	0.023671	5	1.8	0.030771	0.011793	2.5	0.966352	0.640305	0.246613
216.0	1.856678	0.018567	0.018567	216	1.684895	0.117943	0.084245	28	1.8078	0.04863	0.031818	6	1.8	0.052336	0.016355	3	0.804037	0.709562	0.334801
240.0	1.856678	0.018567	0.018567	240	1.61336	0.145202	0.129069	32	1.7755	0.07173	0.041724	7	1.8	0.075044	0.032187	3.5	0.706051	0.746084	0.389175
265.0	1.856678	0.018567	0.018567	265	1.546392	0.170103	0.170103	36	1.7167	0.10867	0.060599	8	1.7	0.11346	0.041856	4	0.582424	0.769324	0.483936
336.0	1.821086	0.036422	0.036422	336	1.328981	0.265796	0.292376	40	1.6668	0.13951	0.079007	9	1.7	0.14391	0.053145	4.5	0.5271	0.785116	0.54091
360.0	1.832797	0.036656	0.018328	360	1.242101	0.285683	0.360209	44	1.6143	0.16692	0.10461	10	1.6	0.18159	0.066418	5	0.449712	0.773011	0.603199
384.5	1.815287	0.036306	0.036306	384.5	1.144119	0.308912	0.434765	48	1.5642	0.19803	0.12357	11	1.6	0.22175	0.08223	5.5	0.401736	0.764463	0.653865
408.5	1.798107	0.053943	0.035962	408.5	1.071026	0.332018	0.481962	52	1.4981	0.23221	0.15581	12	1.5	0.24955	0.10675	6	0.371826	0.743279	0.705279
432.0	1.78125	0.07125	0.035625	432	1.002639	0.350924	0.531398	56	1.4264	0.26531	0.19342	13	1.5	0.30233	0.12198	6.5	0.312744	0.743267	0.753431
504.0	1.715317	0.102919	0.068613	504	0.809199	0.396508	0.679727	60	1.3591	0.29887	0.22724	14	1.4	0.33772	0.1538	7	0.276929	0.732864	0.807192
528.0	1.69997	0.101998	0.084999	528	0.738629	0.39886	0.746015	64	1.2984	0.32628	0.25734	15	1.3	0.37604	0.17834	7.5	0.233751	0.733208	0.835755
552.0	1.670085	0.116906	0.100205	552	0.69973	0.405843	0.7767	68	1.2507	0.3427	0.28992	16	1.2	0.40794	0.23452	8	0.221483	0.718404	0.864693
576.0	1.654092	0.132327	0.099246	576	0.638799	0.408831	0.836826	95	0.97109	0.42806	0.48661	40.5	0.6	0.55898	0.70411	8.5	0.199541	0.704578	0.904438
605.0	1.625784	0.146321	0.113805	605	0.596484	0.423504	0.864902	117	0.77782	0.46662	0.63704	66.5	0.3	0.54039	0.99807	9	0.172455	0.691545	0.945554
672.0	1.533907	0.184069	0.16873	672	0.478951	0.421477	0.98185	141	0.58532	0.49308	0.80365	139	0.1	0.4187	1.3637	9.5	0.156922	0.677481	0.97408
696.5	1.521623	0.182595	0.182595	696.5	0.450344	0.427827	1.004266	166	0.44092	0.50128	0.9325	162	0.0	0.38486	1.4417	10	0.144323	0.654474	1.005856
720.0	1.474392	0.206415	0.206415	720	0.397878	0.429708	1.054377	239.5	0.22666	0.46527	1.1878	186.5	0.0	0.35638	1.476	10.5	0.140115	0.659396	1.01987
744.0	1.440849	0.216127	0.230536	744	0.365338	0.423792	1.09236	262.5	0.1887	0.45152	1.2329	210	0.0	0.32888	1.5176	11	0.122155	0.650195	1.039112
768.0	1.408799	0.225408	0.253584	768	0.337178	0.414729	1.129547	287	0.154	0.43936	1.2794	233.5	0.0	0.30638	1.55	11.5	0.112254	0.64188	1.073587
840.0	1.31975	0.250752	0.31674	840	0.275017	0.407025	1.199074	310.5	0.13017	0.42046	1.3128					12	0.099745	0.576427	1.014906
								334	0.11148	0.40399	1.3458					12.5	0.092192	0.6093	1.119216
																13	0.09158	0.593533	1.139352
																13.5	0.084069	0.590248	1.160908
																14	0.078753	0.578516	1.176957
																14.5	0.07564	0.564274	1.192615
																15	0.073839	0.562728	1.202988
																18	0.052361	0.515543	1.272468
																19	0.057331	0.500561	1.277575
																45	0.013921	0.315718	1.523463
																68	0	0.244438	1.613451
																92	0	0.204585	1.657897

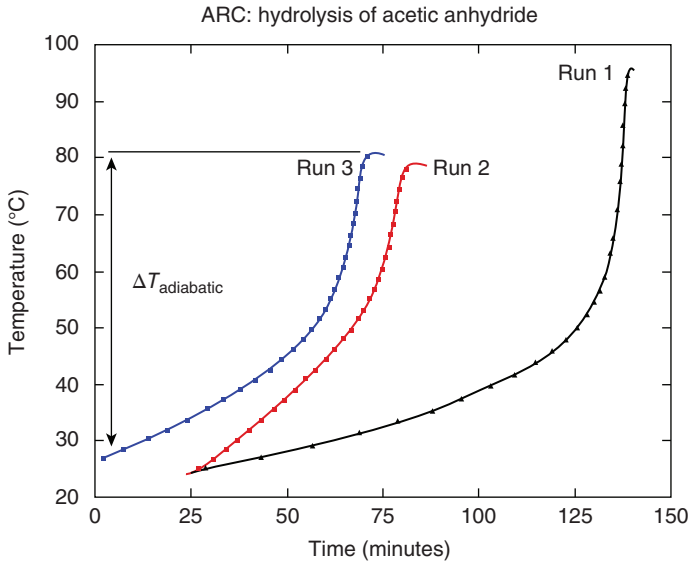

FIGURE 5.B.1 ARC profiles of acetic anhydride injected into water. Given the known heat of hydrolysis of acetic anhydride, the adiabatic temperature rise data was used to validate the PHI.

5.B CALIBRATION FOR PHI FOR ARC ANALYSIS

The PHI factor, ϕ, has been defined as a correction factor applied to time and temperature differences observed in exothermic reactions, which accounts for the sensible heat absorbed by the sample container that would otherwise underestimate ΔH, ΔT_{ad} and result in longer TMR [8].

Mathematically,

$$Ø = 1 + \frac{(mCp)_{container}}{(mCp)_{sample}} \tag{5.B.1}$$

Using ϕ, ARC data can generally be used to calculate ΔH for a process according to Eq. (5.B.2):

$$\Delta H = \phi (mCp)_{sample} \cdot \Delta T_{exp} \tag{5.B.2}$$

where

ΔH is the heat of reaction, decomposition, etc.

ΔT_{exp} is the observed adiabatic temperature rise from experiment

On the other hand, by using a well-characterized reaction with a well-known heat of reaction over a limited temperature range, Eq. (5.B.2) can be rearranged and used to validate ϕ experimentally.

5.B.1 Experimental Discussion

The hydrolysis of acetic anhydride was chosen as a standard reaction for experimentally determining ϕ in the ARC, as it has a well-known ΔH_r^o of 14.01 kcal/mol [9].

Three tests were conducted to evaluate ϕ. In each case a quantity of water was placed into the ARC bomb. The bomb was heated to 25 °C and allowed to equilibrate. Once thermal equilibrium had been established, a quantity of acetic anhydride was injected into the bomb via a syringe through the pressure tube. After the addition, the system was manually placed into EXOTHERM mode to allow for the tracking of the reaction under adiabatic conditions. Using the measure ΔT_{ad}, and averaged specific heat values from the start and end of the experiment, and assuming 100% conversion, ϕ was calculated according from

$$\phi = \frac{\Delta H_{Literature}}{(mCp)\Delta T}$$

5.B.2 Results and Discussion

The results from these experiments are summarized in Table 5.B.1.

In Table 5.B.2 the experimentally determined values of PHI, ϕ, from Table 5.B.1 are compared with values calculated both with and without the Swagelok fittings. Looking at the results in Table 5.B.2, there are three points worth noting:

1. The calculated values for PHI with the fittings included in the mass of the bomb *are more consistent* with the experimentally determined values especially when the sample mass was below 5 g.
2. When the mass of the fittings was omitted, the calculated value of PHI was consistently low, which is undesirable for thermal hazard evaluation as it will lead to an erroneously higher onset temperature and lower heat generation rate.

TABLE 5.B.1 Experiment Summary (ΔH Calculated Based on 14.01 kcal/mol of Anhydride or 58.62 kJ/mol)

Expt. No.	Empty Bomb (g)	Fittings (g)	H_2O (g)	Acetic Anhydride (g)	Mols of Anhydride	Calculated ΔH (J)	Avg Cp of Sample (J/g·°C)	ΔT_{ad} exp (from ARC)	ϕ Calculated from: $\Delta H/mCp\Delta T$
1	10.3955	10.6950	5.2581	4.94	0.0484	2836	3.09	71.43	1.260
2	10.2028	10.7054	2.4794	2.38	0.0233	1366	3.08	54.42	1.678
3	10.4089	10.6520	2.5172	2.66	0.0261	1527	3.02	54.77	1.781

TABLE 5.B.2 Comparison of Experimental ϕ and Calculated PHI with and Without Fittings

Experiment	ϕ Experimental from Table 5.B.1	ϕ Without Fittings[a]	ϕ With Fittings[a]	Mass of Titanium Bomb (g)	Mass of SS Swagelok Fittings (g)
1	1.260	1.166 (7%)	1.336 (–6%)	10.3955	10.6950
2	1.678	1.342 (20%)	1.702 (–1%)	10.2028	10.7054
3	1.781	1.334 (25%)	1.675 (6%)	10.4089	10.6520

[a]Numbers in parentheses indicate deviation from the experimentally determined value. The heat capacity values of both T_i and SS equal 0.12 cal/(g·°C).

3. For the larger sample size experiment (~10 g used in experiment 1), either PHI results in deviations of 6–7%. An average of the two would be closest. But as the sample size is reduced (~5 g), there is a greater deviation and greater error if the fittings are not included in the phi calculation. By including the fittings, PHI was most consistent with the acetic anhydride hydrolysis validations, within 1% for experiment 2 and 6% for experiment 3.

In this work we developed a procedure for estimating PHI directly in the ARC to compare and validate with the two methods of calculating PHI. Based upon these results, it can be generally concluded that the mass and heat capacity of the fittings should be included for low sample masses (<5 g). For this reason PHI values including the fittings were employed in the assessment of ARC data described in this case study since the sample sizes of BTHF used for our ARC studies were typically approximately 4.5 g, and the specific heats were relatively low (~1.7 J/g·°C).

REFERENCES

1. Nettles, S.M., Matos, K., Burkhardt, E.R. et al. (2002). Role of $NaBH_4$ stabilizer in the oxazaborolidine-catalyzed asymmetric reduction of ketones with BH_3-THF. *The Journal of Organic Chemistry* 67: 2970–2976.
2. (a) MARC REISCH (2002). Two seriously injured at Pfizer research site. *Chemical and Engineering News* 80 (27): 11–12. (b) am Ende, D.J. and Vogt, P.F. (2003). Safety notables: information from the literature. *Organic Process Research and Development* 7: 1029–1033.
3. Crowl, D.A. and Louvar, J.F. (2002). *Chemical Process Safety,*, 2e. Upper Saddle River, NJ: Prentice Hall.
4. Burkhardt, E.R., and Corella, J.A. (2000). Borane-THF Complex Method of Storing and Reacting Borane-THF Complex, Mine Safety Appliances Co. US Patent 6,048,985, 11 April 2000.
5. (a) Potyen, M., Josyula, K., Schuck, M. et al. (2007). Borane-THF: new solutions with improved thermal properties and stability. *Organic Process Research and Development* 11: 210–214. (b) Aldrich Technical Bulletin AL-218 (2004). New, safer, amine-stabilized borane-tetrahydrofuran solutions for hydroboration and reduction. Note: 1.0 M BH3-THF, whether stabilized with amines PMP (1,2,2,6,6-pentamethyl-piperidine) or NIMBA (*N*-isopropyl-*N*-methyl-*tert*-butylamine) or with $NaBH_4$, should be stored at 2–8 °C.
6. Monteiro, A.M. and Flanagan, R.C. (2017). Process safety considerations for the use of 1 M borane tetrahydrofuran complex under general purpose plant conditions. *Organic Process Research and Development* 21 (2): 241–246.
7. CCPS (1995). *Guidelines for Chemical Reactivity Evaluation and Application to Process Design*. New York: Center for Chemical Process Safety, AICHE.
8. Townsend, D.I. and Tou, J.C. (1980). Thermal hazard evaluation by an accelerating rate calorimeter. *Thermochimica Acta* 37: 1–30.
9. Wadso, I. (1962). Heats of aminolysis and hydrolysis of some N-acetyl compounds and of acetic anhydride. *Acta Chemica Scandinavica* 16: 471–478.